Center for Advanced Multimodal Mobility Solutions and Education

Project ID: 2022 Project 01

EVALUATING AND COMPARING THE IMPACT OF CONNECTED AND AUTONOMOUS VEHICLES ON CONVENTIONAL INTERSECTIONS AND SUPERSTREETS

Final Report

by

Wei Fan (ORCID ID: https://orcid.org/0000-0001-9815-710X)
Shaojie Liu (ORCID ID: https://orcid.org/0000-0001-5330-3871)

Wei Fan, Ph.D., P.E.
Director, USDOT CAMMSE University Transportation Center
Professor, Department of Civil and Environmental Engineering
The University of North Carolina at Charlotte
EPIC Building, Room 3261, 9201 University City Blvd, Charlotte, NC 28223
Phone: 1-704-687-1222; Email: wfan7@uncc.edu

for

Center for Advanced Multimodal Mobility Solutions and Education
(CAMMSE @ UNC Charlotte)
The University of North Carolina at Charlotte
9201 University City Blvd
Charlotte, NC 28223

September 2022

ACKNOWLEDGEMENTS

This project was funded by the Center for Advanced Multimodal Mobility Solutions and Education (CAMMSE @ UNC Charlotte), one of the Tier I University Transportation Centers that were selected in this nationwide competition, by the Office of the Assistant Secretary for Research and Technology (OST-R), U.S. Department of Transportation (US DOT), under the FAST Act. The authors are also very grateful for all of the time and effort spent by DOT and industry professionals to provide project information that was critical for the successful completion of this study.

DISCLAIMER

TABLE OF CONTENTS

LIST OF FIGURES

LIST OF TABLES

EXECUTIVE SUMMARY

Connected and automated vehicles are currently the new technology and also heighted interests in transportation arena. Many research studies have been done in different aspects of CAVs. In transportation, different modeling frameworks are proposed to ensure that CAVs can travel through the highway, ramps, roundabouts, and most importantly, intersections. For modeling framework, researchers have developed various control strategies to achieve different goals. The modeling topics cover car following models, lane changing models, platooning control of CAVs, platooning control of mixed CAVs and HDVs, trajectory planning of CAVs, platooning-based trajectory planning, and signal optimization, etc. Popular performance indicators, such as travel time, traffic delay, fuel consumption, collisions, and emissions, can be evaluated and significantly improved through numerical simulation on different simulation platforms including PTV VISSIM, SUMO, Paramics and INTEGRATION.

The performances of CAVs in typical transportation environments have been extensively studied, while little attention was given to the performances of CAVs in intersections with innovative designs. In the U.S., numerous innovative intersection designs have been implemented across the country. Such popular innovative intersection designs consist of continuous flow intersection, restricted crossing U turn intersection, and median U turn, etc. Therefore, a research gap exists in evaluating the performances of CAVs on the innovative intersections. This study can mitigate the research gap by simulating CAVs in the environment of fixed signal-controlled superstreet and evaluating relevant performances.

To evaluate the performances of CAVs in fixed signal and adaptive signal-controlled superstreets, this research specifically designs the platooning, trajectory planning and signal optimization models for CAVs. This research also identifies different car following models which could potentially reflect the car following behaviors of HDVs and CAVs respectively. A real-world superstreet is selected and relevant parameters of the HDV-based car following model are calibrated based on the reported traffic flow information. The developed model framework is incorporated into the popular microscopic traffic simulation platform SUMO. Five runs for each simulation scenarios with different traffic demand are conducted to obtain the average traffic delay and fuel consumptions. In addition, this research also tests the performances of CAVs under mixed traffic environments where CAVs and HDVs coexist. An equivalent conventional intersection with a specific lane configuration is also designed in the simulation environment to make a comparison with the superstreet.

The simulation results from calibrated W99 and IDM indicate that IDM with shorter headways yields few benefits in terms of average traffic delay and fuel consumption. Nevertheless, IDM with platooning and trajectory planning can produce less traffic delay and fuel consumption than IDM only in most scenarios. It is also found that platooning and trajectory planning produce quite different impacts in different traffic demand scenarios. The influence of platooning is more significant in heavy traffic volume scenarios while the influence of trajectory planning is more significant in light traffic

volume scenarios. The platooning-based trajectory planning model, in which the trajectory planning is only applied to the leading vehicle of the platoon, produces a balanced performance between trajectory planning and platooning. CAVs under adaptive signal control have a better performance in superstreet compared to trajectory planning and platooning. Trajectory planning model framework could have adverse effects on the fuel consumption in certain traffic volume scenarios as it is lack of consideration of consecutive signalized intersections. The future direction of research can be a more sophisticated trajectory planning model that takes into account multiple closely spaced signalized intersections to alleviate the identified adverse effects.

The simulation results from the mixed traffic environments can yield adverse effects on both traffic delay and fuel consumption. CAVs start to yield benefits when the market penetration rate is 75%. The adaptive signal control can have stable benefits regarding different arm lengths of superstreet.

CHAPTER 1 INTRODUCTION

1.1 Problem Statement

Road congestion has been a major source of economic loss and environmental pollution in the transportation arena. There are different approaches developed by transportation professionals to mitigate this issue, to name a few, signal optimization, innovative intersection design, variable speed limit control, and ramp metering. These methods have been proved to have the ability to significantly improve the performances of existing transportation infrastructure. Among these strategies, innovative intersection design is often featured with a displaced left turn and channelize right of ways. With considerable construction cost, the innovative intersection can significantly increase the traffic efficiency especially when there is relatively large traffic volume from the main road and less traffic volume from the minor road. According to Hummer (2014), there have been numerous superstreets constructed in the states of North Carolina and Maryland. According to the existing investigation on the performances of superstreet, conclusions were made that superstreet can provide both travel time and safety benefits. Nevertheless, it was also pinpointed that superstreet may confuse drivers who are not familiar with superstreet designs. Hence, in the implementation stage, proper road signs and signal indications play important roles in the superstreet operations.

Recently, as a new technology trend, connected and autonomous vehicles have come to reality thanks to the development of information and computation technologies. Many researchers have devoted their efforts to investigating the benefits of CAVs in different transportation environments, including freeways, ramps, roundabouts, and intersections. Nevertheless, the knowledge on the performances of CAV in the innovative intersection design is limited. The lack of this knowledge may produce biased prediction on the future influence of CAVs in the existing transportation infrastructure. Hence this research is designed to mitigate this gap by evaluating and comparing the performance difference of the superstreet and conventional intersection.

In these studies, advanced CAV behavior models are developed and tested against traditional HDVs such as trajectory planning and platooning. The mechanisms of trajectory planning vary in different transportation settings. For example, in the signal-controlled intersection, trajectory planning relies on the communication of vehicles and traffic signal controllers. On the other hand, in the non-signalized intersection, the trajectory planning will rely on communication with other vehicles so that the optimal sequence of entering the intersection can be planned. In addition, car-following models of CAVs often differ from the ones of HDVs. The car-following models of CAVs have an intuitively measurable parameter, whose values are made feasible through Radar or LiDAR of CAVs. Platooning and adaptive signal control are two advanced CAV features which rely on vehicle to vehicle (V2V) and vehicle to infrastructure (V2I) communication technologies. This project also develops relevant models to test these CAV features in the superstreet environment.

1.2 Expected Contribution

To test the performances of CAVs in superstreet and conventional intersections, this research calibrates HDV models and develops specific models for CAVs. The contribution of this research includes the following:

1. Developed platooning, trajectory planning, and adaptive signal controls for CAVs.
2. Calibrated W99 model for HDVs in the environment of superstreet.
3. Identified the impact of CAVs in the environment of superstreet and conventional intersection with each standalone features.
4. Conducted sensitivity analyses for CAV models in specific scenarios.

1.3 Report Overview

Chapter 1 provides essential background information about CAVs and superstreets in the problem statement and motivation section. This chapter also covers the research objectives and expected contributions from this research. In the end, Chapter 1 describes the overall research structure for this study.

Chapter 2 presents a comprehensive review of the existing literature on the behavior models for CAVs and HDVs as well as superstreets. The behavior models for simulated vehicles can be grouped into four categories, which are intersection management, car following, lane changing, and CAV platooning. The intersection management section reviews how CAV behave in non-signalized intersections and signal-controlled intersections respectively. For the superstreet, this chapter presents the concept and application of the superstreet design, existing studies on the operational performance of superstreet, and research on the CAVs and superstreet.

Chapter 3 illustrates the methodologies and the overall experiment framework. First, this chapter introduces the behavior models employed in this research, including Wiedemann 99 (W99) and Intelligent Driver Model (IDM), platooning control, trajectory planning, adaptive signal control, and trajectory planning under adaptive signal control, followed by the description of the simulation platform. Two sets of platooning controls and trajectory planning controls are developed and tested respectively. The research team also applies different car following models for HDVs and CAVs to distinguish their characteristics. Sensitivity analyses, such as traffic scales, market penetration, and arm lengths from superstreet, are conducted in some specific scenarios. Chapter 3 also covers the information about the selected real-world superstreet and the designed simulation experiments.

Chapter 4 presents the simulation results for the operational performances of CAVs and HDVs in the environment of the superstreet and the equivalent conventional intersection in terms of average traffic delay and fuel consumption. According to the designed scenarios in Chapter 3, the effects of each CAV technique are validated by the corresponding simulation results. This chapter also provides relevant rationales for the different performances with CAV techniques and in different environments. Traffic

delays and fuel consumption are selected as the performance indicators since they can represent the transportation efficiency and environmental impacts respectively.

Chapter 5 concludes this research with the main findings from this research. These findings may provide important references for policymakers or transportation designers. The control strategies devised to obtain these findings can also be utilized for other CAV studies. In addition, this chapter also discusses the potential future research directions that are highly related to the current research topic.

CHAPTER 2 LITERATURE REVIEW

The literature review section covers several topics, including superstreets, car-following models for CAVs and HDVs, platooning of CAVs, trajectory planning for CAVs, and signal optimization with CAVs. The literature view section provides a solid reference for the later-proposed model framework of CAV behavior models. With the proposed CAV model framework, the performances of CAVs in the environment of superstreet and conventional intersections can be well represented.

2.1 Superstreet Background and Relevant Studies

2.1.1 Superstreet Background

Superstreet is one of the popular innovative intersection designs. It has superior performance compared to the conventional intersections in unbalanced traffic volume scenarios, which is often seen in the real world. It is a variation of the median U-turn design, which guides left-turn vehicles from both the main street and minor street to travel through the intersection first and make a U-turn in a median opening that is usually situated hundreds of feet away from the main intersection. Superstreet differs from the median U-turn design in that left-turn vehicles from the main street can avoid making a U-turn by going through a dedicated channel to further increase the traffic efficiency for the main street. Unlike the median U-turn design, through movement from the minor approaches in the superstreet also have to make the detour in the median opening to complete the trip. With such design, superstreet can increase road capacity and enhance safety due to the fewer number of phases and conflicting movements in each sub intersection of the superstreet environment.

Superstreet has been successfully implemented in numerous states in the US (Hummer et al., 2014) and researchers have also investigated the performances of superstreet in various aspects including safety, travel time, traffic delay, and so forth (Haley et al., 2011; Hummer et al., 2010; Naghawi and Idewu, et al., 2014; Ott et al., 2015; Reid and Hummer, 2001). Conclusions were made that the superstreet can outperform the equivalent conventional intersections in terms of average travel time or traffic delay.

For safety benefits, in addition, the design of the superstreet successfully reduces the conflict points inside the superstreet system compared to the conventional intersection. Nevertheless, it should also be noted that the design of the superstreet may confuse drivers who are not familiar with superstreet. Such a phenomenon may impact the safety benefits of superstreet adversely.

Apart from the performance and safety studies, Xu et al. (2017) investigated the optimal U-turn offset length with an analytical approach based on the drivers' acceptable gap distributions. Later, Xu et al. (2019) investigated the optimal signal timing design for superstreet with the objectives of maximizing the throughput and green bandwidth. Both of these studies provided important references for the application of superstreets.

Although there have been few studies that have been identified with both topics of CAVs and innovative intersection, Zhong et al. (2017) studied the CAV performances in diverging diamond interchange and superstreet respectively.

2.1.2 CAV in Different Environments

Extensive efforts have been made to evaluate the performance of CAVs in various typical transportation environments, including freeway segments, conventional intersections, and roundabouts. A sample of literature for the CAVs studies in other transportation environments is provided in Table 2.1. CAVs outperformed the HDVs in various transportation environments.

TABLE 2.1 CAV Studies in Other Transpiration Environments

Transportation Environments	Authors	Year	CAV Features
Freeway	Guo, J. et al.	2020	CACC, platoons, cooperative merging
	Adebisi et al.	2020	CACC models
	Liu and Fan	2020	CAVs with revised intelligent Driver Model
	Chityala et al.	2020	CAVs with shorter headways
	Hu and Sun	2019	Cooperative Lane Changing Control, Cooperative Merging Control
Conventional Intersection	Han et al.	2020	Platooning based Trajectory Planning with optimal control framework
	Pourmehrab et al.	2020	CAVs with an intelligent intersection control algorithm (IICA) and hybrid autonomous intersection management (H-AIM)
	Guo, Y. et al.	2019	Joint optimization of vehicle trajectory and intersection controller with combined dynamic programming and shooting heuristic approach
Roundabout	Mohebifard and Hajbabaie	2020	CAVs with optimized trajectory
	Mohebifard and Hajbabaie	2021	Trajectory control in a roundabout with a mixed fleet of automated and human-driven vehicles
	Martin-Gasulla and Elefteriadou	2021	Roundabout management algorithm for trajectory planning of CAVs
	Chalaki et al.	2020	Trajectory planning control framework for roundabout

2.2 Car Following Models

This section introduces the popular models in modeling CAVs and HDVs respectively. CAV car following models include IDM, Adaptive Cruising Control (ACC) model, and Cooperative Adaptive Cruising Control (CACC) while the HDV car following model mainly discusses the W99 model. A brief literature summary is provided in Table 2.2 for the studies that have considered IDM, ACC, or CACC in their CAV research.

TABLE 2.2 Applications of IDM, ACC, and CACC Models

Kesting and Treiber	2008	IDM	Applied the genetic algorithm to optimize the parameters in IDM using trajectory data
Moon et al	2009	ACC	Design, tuning, and evaluation of a full range ACC system with collision avoidance control.
Nowakowski et al	2010	CACC	Surveyed 16 drivers on their acceptability of CACC system
Bifulco et al	2013	ACC	Proposed four-layer structure ACC control system for automated vehicles.
Derbel	2013	IDM	Improved IDMby guaranteeing traffic safety and reducing the overly high deceleration
Milanes et al	2014	CACC	Presented the design, development, implementation, and testing of a CACC system
Ploeg et al.	2014	CACC	Evaluate string stability behaviors through theoretical analysis on the wireless inter-vehicle communication to provide real-time information of the preceding vehicle
Rachel M. Malinauskas	2014	IDM	Examined the IDM in the vector-valued time-autonomous ODE system
Treiber et al.	2017	IDM	Added external noise and action points to the IDM

2.2.1 IDM

The Intelligent Driver Model, i.e., IDM, was developed by Treiber (2000) firstly to model the traffic in a single lane without considering the lane changing behavior. IDM has intuitively measurable parameters which can be easily accessed through the communications between vehicles and infrastructures. All six parameters have concrete meaning (Kesting and Treiber, 2008). IDM provides a good foundation for researchers to further develop the ACC vehicle model or CACC model. Therefore, it is popularly applied in modeling CAVs. There are currently a considerable number of studies that have chosen IDM as the base model for CAV behaviors, as shown in Table 2.2.

2.2.2 ACC and CACC

Adaptive Cruising Control model is developed to model the CAVs without communication capability with other vehicles. Nevertheless, ACC vehicles can detect the distance and velocity through Lidar but with an increased delay compared to the vehicles that can communicate with other vehicles directly.

ACC is a terminology that describes the longitudinal control strategy for autonomous vehicles that have radar, lidar, and camera installed. Many of these longitudinal control strategies are distance regulation oriented (Shladover, 1995; Xiao et al., 2011). According to He et al. (2019), the ACC models can be classified as proportional-integral-derivative (PID) feedback/feedforward control, model predictive control (MPC), and fuzzy logic control (FLC). PID control is a commonly accepted and tested strategy for ACC and a representative is a model proposed by Shladover et al (2012), in which the acceleration rate of the following vehicle was expressed as a function of the distance error and the relative speed. Geiger et al. (2012) developed a CACC system (which covers the functions of ACC) based on the MDC. By assuming the preceding vehicle drive at constant yaw rate and acceleration in the defined time horizon,

the optimal acceleration rate is obtained by minimizing the cost function which contains the terms of distance error, relative speed difference, and the current acceleration rate. FLC resolves the ACC problem by calculating the safe distance depending on whether a preceding vehicle is present or not.

CACC improves ACC by adding communication between vehicles. For ACC vehicles, the information on the preceding vehicle is retrieved by onboard sensors like radar or lidar. CACC vehicles can share the speed, position, and acceleration rate with shorter communication latencies. CACC control and ACC shared a similar model structure in Xiao et al. (2017) but had shorter reaction time and spacing margins.

Arem (2006) studied the impacts of CACC for a highway-merging scenario from four to three lanes. The CACC system was modeled with the traffic flow simulation model, MIXIC. MIXIC was utilized to control the longitudinal movement of CAVs when CACC mode was not in control. The simulation results showed an improvement of traffic flow stability with a slight increase in traffic-flow efficiency compared to vehicles without CACC control.

To sum up, IDM, ACC, and CACC are all popularly applied in CAV modeling for their intuitive measurable parameters. These three models are also in continuous developing stages for addressing limitations with technology development. In addition to these models, there are also other car-following models applied in CAV research, such as Newell's car-following model. Newell's car-following model is appealing in modeling CAVs for its simplicity and consistency with the triangular fundamental diagram, by giving the exact numerical solution for the kinematic wave model (Chen et al., 2012). Numerous researchers have applied Newell's car following model in their trajectory optimization or platooning models (Gong and Du et al., 2018; Wei et al., 2017).

2.2.3 W99

2.2.3.1 Brief Overview for the HDV Car Following Model

When transportation professionals evaluate proposed intersection designs or signal designs, simulation environments are often employed. The embedded car following model in the simulation software is often utilized as the HDV car following model by default. Table 2.3 provides a summary of the popular car-following models and their associated car-following models. In the PTV VISSIM, Wiednesmann 1974 and W99 are the only two models supported by default. However, PTV VISSIM allows users to add user-defined car following model through Application Programming Interface (API). For AIMSUN, the car following model is developed based on Gipp's car-following model. PTV VISSIM and Paramic both employed a psychophysical car model which could capture the randomness of the human drivers' behaviors.

TABLE 2.3 Microscopic Traffic Simulation Software and Their Involved Car following Model

Software	Car following model involved
PTV VISSIM	Wiedesmann 99 and Wiedesmann 1974
AIMSUN	Gipps
MITSIM	GHR model
Paramics	Fritzsche pscho-physcial model
INTEGRATION	Pipes model

2.2.3.2 W99 Illustration

W99 model, or the Wiedemann 99 model (ten parameter version), belongs to the psychophysical or action point models. The driving behavior of humans is assumed to be normally distributed, which indicates that each driver has a different perception, reaction, and estimation of surrounding traffic environments, safety needs, desired speed, and aggressiveness towards maximum acceleration/deceleration values (Ahmed et al., 2021). In the Wiedemann model, CAVs would have four modes, namely the following behavior, free driving behavior, closing-in behavior, and breaking behaviors. All these behaviors are modeled with different function that also contains parameters for calibration.

The W99 model is employed in the popular simulation platform, PTV VISSIM. Through the W99 model and PTV VISSIM, many transportation researchers had employed W99 to calibrate HDV traffic for their studies or assume default values of W99 in their evaluations of traffic performances.

Kaths et al. (2021) employed the W99 model to calibrate the bicycle traffic characteristics in PTV VISSIM. The calibrated model was validated with trajectories collected during a bicycle simulator experiment. The trajectory data contained the position and velocity for each simulation step. The simulation results indicated that average queue dissipation time decreases as the width of the bicycle lane increases. The validation results showed that a 1.5 m wide bicycle lane was the most meaningful in assessing the car-following model parameters.

Durrani et al. (2016) calibrated W99 for three vehicle classes, i.e., cars, heavy vehicles, and motorcycles. A total of 2160 vehicle trajectories were obtained from a 640-m segment of US-101 in Los Angeles, California in the morning peak hour. Different sets of control parameters of W99 were calibrated for these three vehicle types and it was found that the driving behaviors of cars and heavy vehicles are significantly different. For example, heavy vehicles had a longer spacing time gap compared to cars. The difference between simulated and observed average speed and acceleration distributions were the calibration goals to be minimized.

Chaudhari et al. (2022) proposed a calibration approach for the W99 model in the mixed traffic composition scenarios, where six classes of conventional vehicles were present, including motorized two shellers, cars, auto/three-wheelers, buses, light commercial vehicles, and heavy commercial vehicles. This research also modified the acceleration equations of the existing W99 model to better represent the mixed traffic

conditions. The calibration approach and performance were both tested. The modified W99 had a smaller root mean square error (RMSE) compared to the existing W99.

2.3 Platooning

2.3.1 Introduction

In the CAV environment, a platoon is defined as a group of vehicles that include a leader, which leads the platoon on the road, and followers, which follow their preceding vehicles with a short distance (Hallé and Chaib-draa, 2005). There have been a considerable number of studies that have investigated the potential benefits of platooning feature of CAVs, such as reducing congestion, increasing capacity, and alleviating pollution. When CAVs are inside a platoon, they can maintain smaller headways compared to non-platooning vehicles. The platooning feature of CAVs can also reduce the operational cost of commercial truck companies when the behaviors of the following trucks are determined by the leading trucks (Hurtado-Beltran and Rilett, 2021). Because of the benefits mentioned above, CAV platooning is a subject of heightened interest for the industry sector. Bhoopalam et al. (2017) comprehensively reviewed the existing literature on truck platoons and discussed the future research directions. Bevly et al. (2017) examined the feasibility of implementing driver-assisted truck platooning schemes with cooperative adaptive cruise control. It was found that truck platooning can successfully reduce fuel consumption by 5% - 7%.

2.3.2 Platooning Behavior Models

Platooning is a unique behavior feature of connected vehicles that can communicate with surrounding vehicles. Different from the automated vehicles that detect the gap and velocity of preceding vehicles, connected vehicles share the velocity and acceleration rate of the vehicles. With such communication capability, CAVs can have shorter reaction times and headways, which can further reduce fuel consumption. (Xiao et al., 2016). Xiao et al. (2017) developed the CACC model to describe the car following behaviors of CAVs that can communicate with each other. However, the CACC model form only loosens platoons. Differing from this approach, several researchers developed car following behavior for vehicles inside platoons specifically.

2.3.2.1 Virtual Platoon

Some studies conveniently defined the platoon as the group of vehicles that travel through the intersections together or share a close headway.

Feng et al. (2018) and Yu et al. (2018) developed a signal optimization scheme and trajectory planning scheme for CAVs in the convention intersections. They defined the vehicle platoons as a group of vehicles that can travel through the intersections. In this way, the vehicles that can pass the intersections entered the trajectory planning module together.

Ye et al. (2019) identified the vehicle platoons by their inter-distance and speeds. When the vehicles are close to each other and share a similar speed, they are grouped into a platoon for trajectory optimization whose aim is to minimize fuel consumption. With such a module, the computation burden is reduced since a group of vehicles can be regarded as a single unity for the trajectory optimization process.

2.3.2.2 Optimized-based Platoon

Wang et al (2020) established an MPC approach to model the platooning behaviors of CAVs. In this research, two solutions were proposed to obtain the optimal trajectories for vehicles inside a platoon and the solutions were applicable in real-world tests. Such a method can significantly reduce the computation time and improve the control efficiency according to the simulation results. In the case study, the CAV platoon whose leading vehicle's trajectory was obtained from field data. The results demonstrated that the proposed model framework can dampen traffic oscillations efficiently and smooth the deceleration and acceleration behaviors for all following vehicles inside the platoon.

Xiong et al (2021) developed a coordinated platooning strategy using a Markov decision process formulation. The optimal coordination strategy was threshold-based. A recursive approximation algorithm was proposed to compute the optimal strategy, which is superior to the generic value iteration algorithm. This strategy was also validated through traffic data.

Utilizing the distributed algorithm for multi-users proposed by Koshal et al (2011), Gong et al. (2016) analyzed and obtained the solution for the optimization problem of CAV platoon control. The distributed algorithm was proved to provide the solutions efficiently for the control problem. Then this control strategy was demonstrated through extensive numerical simulations.

Later, Gong and Du (2018) proposed a cooperative platoon control strategy for mixed traffic flow where CAV and HDV coexist. The movement of CAVs was controlled by One- or P- step model predictive control (MPC) models while the HDVs were modeled by the well-accepted Newell car-following models. Gong and Du (2018) also developed an online curve matching algorithm to anticipate the aggregated response delay of the HDVs. The MPC problem was solved by a distributed algorithm proposed by the authors. The numerical studies proved that the proposed algorithm can solve the One-step and P-step MPCs problems quickly. Finally, the authors demonstrated that this cooperative platoon control strategy is superior to the non-cooperative control strategy and a latest CACC strategy.

Dynamic programming was also employed in the platooning control of CAVs. Wei et al. (2017) established a novel control strategy and a family of efficient optimization models as well as algorithms to solve efficiently semi-open boundary conditions. The methods belong to the Proportional-Integral-Derivative (PID) category, in which the control input of an individual vehicle is calculated from a linear or nonlinear

function. The test results of the proposed model framework in different bottleneck scenarios revealed the efficiency of the proposed model and controlling reaction time as a new control variable.

2.3.2.3 Model-based Platoon

Bang and Ahn (2017) developed platooning scheme based on the spring-mass-damper system. The acceleration rate was a function of the velocity of the preceding vehicle and the leading vehicle, and the positions in the platoons. The differences were weighted by the spring constant and damping coefficient respectively. The valid domains of control parameters were derived based on vehicles' physical properties. This research also tested the different relationships between the control parameters and traffic flow, including maximum, quadratic, and cubic spring constants. The results showed that the maximum spring constant and flow with critical damping have the most efficient platooning. A cubic spring constant was desirable in light traffic conditions to allow proper lane changing.

Rajamani et al. (2012) proposed a vehicle platooning controller that has been well accepted (Bian et al., 2019; Darbha et al., 2017; Darbha et al., 2018; Paden et al., 2016). With the same platooning control structure, Darbha et al. (2017, 2018) verified the minimum headway requirements in different connection levels (how much predecessor information can be received and whether the acceleration information is available). Bian et al. (2019) further proved that a platoon can be asymptotically and string stable when the time headway was lower-bounded, and this boundary could be reduced when more predecessors' information was available. Overall, the popular safety assumption was that the minimum headway should be two times the communication delay, and CAV platooning could yield benefits when the minimum headway is less than 1s (Darbha et al., 2018).

2.3.2 Platooning Size

The length of vehicle platooning is another research topic that receives considerable attention. When the vehicle platoon is traveling through the intersection, the number of vehicles that can pass through the intersection is limited, and the optimal number of vehicles that can pass through the intersection needs to be determined to avoid collisions or emergency brakes. Nevertheless, there is little research that has investigated platooning size. In the environment of the freeway, there is often no limitation on the platoon size. However, when CAVs are traveling through the intersection, the platoon size may not be exceedingly long to travel through the intersection.

Zhao et al. (2018) developed a cooperative platooning control strategy for CAVs in terms of longitudinal movement on the urban road. This research tested different platoon sizes of CAVs including sizes of 1, 2, and 5 respectively. Considering the calculation burden and communication reliability in practice, the author set the maximum number of platoon sizes to be 5. When the maximum platoon size was 1, the longitudinal trajectory only considered the individual vehicle. When the maximum platoon size was 2,

the optimization control only considered the fuel consumption of the subject vehicle and its direct following vehicle. When the maximum platoon size was 5, the optimization control was applied on the subject vehicle and its direct 4 following vehicles. The results showed that then overall performance was better when the maximum platoon size is larger.

Guo and Ma (2021) tested the CACC control framework proposed by Liu et al. (2018) in the environment of the signalized corridor. This research examined the platooning performance with different maximum platoon lengths. The researchers tested the performance of 1, 3, 5, 8 and 10, and the results showed that a maximum platoon length of 10 yielded the largest throughput and minimal traffic delay.

2.4 Trajectory Planning

2.4.1 Introduction

CAVs with trajectory guidance capabilities can travel on the road with certain optimal traffic measures such as fuel consumption, emissions, and fuel consumption. The trajectory planning problem is often formulated as an optimal control problem. The solution towards the optimal control problem often results in a non-linear optimization problem that can only be solved by either nonlinear programming methods or metaheuristic methods such as the genetic algorithm. Nevertheless, these methods inevitably bring challenges in real-world applications as significant computation resources may be required when the traffic demand is large.

2.4.2 Pontryagin Minimum Principle Approach

Wan et al., 2016

The trajectory planning problems of CAVs usually took the minimizations of traffic efficiency and environmental impacts into consideration as the objectives. Wan et al. (2016) analyzed the property of the objective function through Pontragin Minimum Principles (PMP) and concluded that the optimal trajectories are bang-singular-bang control, which resulted in three segment speed trajectories. This research applied a two-segment trajectory in which the vehicle first accelerates or decelerates to the target final speed and then cruises at the final speed to go through the intersection. This research employed the proposed trajectory planning strategy in the simulation platform, Paramics, and found that CAVs not only reduce their fuel consumption but also help to reduce the fuel consumption of other conventional vehicles. Nevertheless, the improvement in fuel economy was achieved with a little compromise in average traffic flow and travel time.

Feng et al. 2018

Feng et al. (2018) proposed an analytical approach to minimize the accumulated acceleration rates when CAVs were approaching the intersection. The optimal solution generally resulted in a three-segment trajectory, in which CAVs keep a constant speed in

the second segment and a constant maximum acceleration/deceleration rate in the first and third segments. The transition time point could be easily determined given the final time step, final speed, and initial speed. The proposed trajectory planning modeling framework was proved efficient through simulation tests under adaptive signal-controlled intersections. In the adaptive signal-controlled intersection, the traffic delay and fuel consumption were both reduced. The adaptive signal was controlled by the developed dynamic programming algorithm. The dynamic programming aimed to minimize the average travel time of CAVs. Moreover, this research also identified the proper maximum acceleration/deceleration rate in this research, which was 1.5 m/s. Also, trajectory planning was conducted on the leading vehicle of the defined platoon. The platoon was defined as the group of vehicles that can travel through the intersection within the same phase.

Yu et al. 2018

Building on Feng et al. (2018), Yu et al. (2018) proposed a mixed-integer linear programming method to optimize the trajectory and signal timing simultaneously. The optimization framework first incorporated the lane-changing movement. Vehicles were also split into platoons and were guaranteed to pass through the intersection at the desired speed. The simulation results demonstrated that the proposed actuated vehicle control framework could successfully reduce carbon dioxide emissions and traffic delays. In addition, the road capacity was also increased. This research also conducted a sensitivity analysis in the no-changing zones on the optimality of the proposed model.

2.4.3 MDP Approach

Zhao et al. 2018

Model predictive control (MPC) is the popular approach to solving the trajectory planning problem of CAVs. Zhao et al. (2018) utilized this method to test CAV performances in an urban intersection with assumed different traffic demands. The trajectory planning strategy aimed to minimize the fuel consumption at the same time while ensuring the vehicle travel through the intersection at maximum speed. The resulting problem was then solved by Gauss pseudospectral method in the GPOPS package from MATLAB. Utilizing the proposed methods, the authors analyzed the properties of CAVs with different capabilities with small traffic scales. This method may nevertheless encounter challenges in applications as significant delays may occur in obtaining the optimized trajectories.

2.4.4 Heuristic Approach

Kamalanathsharma et al. 2015

Green Light Optimal Speed Advisory system (GLOSA) is a system in the CAV environments where vehicles can continuously be guided at an optimal speed. Kamalanathsharma et al. (2015) extended the GLOSA system to a variable speed limit for each vehicle to minimize fuel consumption. This research utilized the Virginia Tech Comprehensive Power-Based Fuel Consumption Model (VT-CPFM) to obtain the fuel consumption instantaneously. The optimal speed limits for each vehicle were determined

by a dynamic programming algorithm and further incorporated into INTEGRATION (popular simulation software). The simulation results demonstrated the efficiency of the proposed modeling framework.

Zhou et al., 2016 and Ma et al. 2016

A parsimonious shooting heuristic method was proposed by Zhou et al. and Ma et al. Zhou et al. (2016) constructed the optimal control model framework and Ma et al. devised an efficient algorithm to solve the optimal control problem. Zhou et al (2016) proposed a systematic approach to obtain the optimal trajectories for CAVs approaching the urban signalized section considering kinematic limits, traffic arrival patterns, car following safety, and signal operations. A numerical sub-gradient-based algorithm with a shooting heuristic was developed to solve the proposed optimal control problem. Numerical experiments were conducted, and the results showed that the vehicle's trajectories generated from the proposed method considerably outperform the ones from human drivers in terms of travel time, fuel consumption, and safety risk.

Zhou et al. 2020

Zhao et al. (2020) tested the CAV performances with different communication ranges. The CAVs were controlled with a bilevel optimization algorithm so that minimal traffic delay could be achieved when the CAVs were traveling through the intersection. The communication ranged from 100m to 500m with an interval of 100m. The results showed that the operational performances are better when the communication ranges were longer after 200m, which suggested that the communication range should be at least 300m to ensure the traffic flow operates stably. The CAVs were also enabled with the platooning system, and the maximum number of platoons that can pass the intersection was identified when the communication range is 100m.

Guo and Ma 2021

The management framework of the signalized corridor with CAVs has also attracted certain interests. Guo and Ma (2021) introduced signal control and trajectory control with CAVs. In addition, this research also implemented the platooning concept for CAVs. The platooning control logic followed the work of Liu et al. (2018), in which CAVs switched to the CACC model when the distance to the preceding vehicle is less than 120 meters. Once the simulation started, the platooning control logic would initiate, and vehicles in the platoon started to run with CACC control. Then the trajectory of the leader vehicle was optimized with stage-wise trajectory control procedures, which was similar to Feng et al (2018) and Yu et al. (2018). An adaptive signal control was also proposed which essentially provided green extension when necessary. These models were tested in a corridor of three consecutive signalized intersections and the results showed that the traffic delay can be reduced compared to the benchmark scenarios. It was concluded that platooning is the most effective individual operational because it directly reduced the gaps between vehicles. Sensitivity analysis was conducted on the market penetration rate and platooning length.

2.4.5 Artificial Intelligence Approach

Cheng et al. 2022

Cheng et al. (2022) proposed a deep reinforcement learning approach to design the trajectory of CAVs in a mixed traffic environment where both CAVs and HDVs existed. The reinforcement learning approach was one of the popular machine learning methods that can be utilized in the optimal control problem. This approach had two important concepts, state, and action. The state represented the external environment that the smart agent was situated in and the action was the available actions that the smart agent could take. In the trajectory optimization problem, the smart agent was each CAV running on the road and the state could be the distance to the intersection, signal status, or else. The action was the acceleration rate of the subject vehicles and was associated with a reward. The reward was maximized through the neural network learning process in the work of Cheng et al. (2022). The simulation results showed that the proposed methods could reduce fuel consumption by 7.8% in a fixed signal timing.

2.5 Signal Optimization under CAV Environments

When vehicles are equipped with CAV technologies, it is convenient to assume the communication between CAV and signalized intersections. While signalized intersections optimize its phase duration and sequence, CAV can adjust trajectories based on its updated signal timing to improve the performance indicators. Currently, there are different methodology trends in terms of optimizing the signal timing. According to Qadri et al., (2020), these methods can be grouped into five categories, including artificial intelligence models, metaheuristics-based approaches, multi-objective-based approaches, dynamic/mixed-integer programming (MIP) based approaches, and miscellaneous approaches. Each of these approaches could further grow its branches. For example, artificial intelligence approaches could have neural network models and deep learning models. This research intended to employ a MIP-based approach to develop a signal optimization model, hence a review of existing studies for MIP-based signal optimization was summarized in Table 2.4. According to Table 2.4, it can be observed that the cell transmission model, Space-Phase-Time Hypernetwork based model, and green start/duration mixed-integer programming models are three popular approaches when modeling signal optimization problems.

Table 2.4: Recent Studies on Signal Optimization with MILP Approaches

Title	Important assumption	Authors	Year
An Enhanced 0–1 Mixed-Integer LP Formulation for Traffic Signal Control	Cell Transmission Model	Lin et al.	2004
Distributed optimization and coordination algorithms for dynamic speed optimization of connected and autonomous vehicles in urban street networks	Cell Transmission Model	Tajalli, and Hajbabaie	2018
A novel traffic signal control formulation	Cell Transmission Model	Hong K. Lo	1999
A Cell-Based Traffic Control Formulation: Strategies and Benefits of Dynamic Timing Plans	Cell Transmission Model	Hong K. Lo	2001
Recasting and optimizing intersection automation as a connected-and-automated-vehicle (CAV) scheduling	Space-Phase-Time Hypernetwork	Li and Zhou	2017

problem: A sequential branch-and-bound search approach in phase-time-traffic hypernetwork			
Solving simultaneous route guidance and traffic signal optimization problem using space-phase-time hypernetwork	Space-Phase-Time Hypernetwork	Li et al.	2015
A mixed-integer programming formulation and scalable solution algorithms for traffic control coordination across multiple intersections based on vehicle space-time trajectories	Space-Phase-Time Hypernetwork	Wang et al.	2020
Collaborative control of traffic signal and variable guiding lane for isolated intersection under connected and automated vehicle environment	Green start and duration MIP	Ding et al	2021
A Platoon-Based Adaptive Signal Control Method with Connected Vehicle Technology	Green start and duration MIP	Li, et al.	2020

2.5.1 Cell Transmission Model

The cell transmission model was derived from Lighthill, Whitham, and Richards (LWR) model, which describes the dynamic relationship among traffic flow, density with respect to space, and time variables. Later, Daganzo (1994, 1995) proposed a simplified solution by assuming the traffic flow equals the minimum of three norms, i.e., the product of free speed and current density, inflow capacity, and the product of backward shock wave speed, and the difference between jam density and current density. Based on this formulation, the traffic delay was represented by the differences between the numbers of vehicles that had been left in the current cell between two successive time steps. The flow at the next time step could be equal to the saturated flow rate when the signal was green, and zero when the signal was red.

Through the equations introduced above, researchers can easily construct a mixed-integer linear programming problem for the signal optimization problem (Hong K. Lo, 1999; Hong K. Lo, 2001; Lin and Wang 2004). However, this approach became unsuitable when it comes to the microscopic operation level, as it often involves a relatively larger simulation resolution (simulation step of 10s).

2.5.2 Space-Phase-Time Hypernetwork Model

Li et al. (2015) established a new approach to optimizing the traffic signals at in-network levels. In this signal optimization, each link in the network was expanded from one dimension to two dimensions considering both the position and time step for each vehicle in the planning horizon. Each link was associated with a calculated cost that is largely determined by the travel time with free speed at the current time step within the horizon. Similar assumptions were also implemented for signal phases. All possible signal phases were expanded in the given planning horizon and represented by nodes. These graphical representations for the links and phases enabled researchers to establish the signal optimization model that was convenient for Lagrange relaxation. The derived formulations from Lagrange relaxation could be solved by either branch and bound algorithm or dynamic programming (Li and Zhou 2017; Li et al., 2015).

2.5.3 Green Start and Green Duration-based MIP

Another popular approach for signal optimization is to optimize signal timing by taking the green start and green duration as the decision variable for each phase in an MLP model. In a connected environment, signal controllers are assumed to receive the estimated arrival information, and hence the traffic delay can be easily estimated by calculating the difference between the green start time and vehicle arrival time.

Li et al (2020) constructed a signal optimization for the NEMA phase with a dual-ring structure. The phase boundaries and sequences were modeled as constraints in the MILP model and the objective was to minimize the traffic delay. One of the highlights in this research is that the researchers considered the arrival times of platoons instead of individual vehicles. However, the signal optimization model still yielded a signal timing plan with a fixed number of phases and phase sequence, which may limit the signal timing performance.

Similarly, Ding et al (2021) also developed a signal timing optimization model in the connected environment with green start time and green duration as the decision variables. Particularly, this research selected the wasted green time as the objective to be minimized. The wasted green time was defined as the time difference between vehicle arrival time and green start, as described below. One of the merits of the model developed by Ding et al (2021) was that the phase sequence is flexible because of the introduction of the auxiliary binary variable indicating which phase was first between conflicting phases.

CHAPTER 3 METHODOLOGY

3.1 Introduction

Based on the literature review, it can be seen that the behaviors of CAVs require specific models to describe. This chapter attempts to model the car following, platooning, trajectory planning, and adaptive signal control. The following subsections provide more details about these models.

3.2 Car-following Models

3.2.1 IDM

IDM was developed by Treiber et al. (2000). It is a collision-free model with intuitively measurable parameters. Due to these advantages, the IDM has been popularly used in modeling CAVs (Do et al., 2019; Liu and Fan, 2020; Yi et al., 2020). The acceleration rate in IDM is a function of the velocity of the subject vehicle, the gap to the preceding vehicle, and the velocity difference to the preceding vehicle, as Equation 3.2.1.1 and Equation 3.2.1.2 show below:

$$a(s, v, \Delta v) = a_m \left(1 - \left(\frac{v}{v_d} \right)^{\propto} - \left(\frac{s^*(v, \Delta v)}{s} \right)^2 \right) \quad (3.2.1.1)$$

$$s^*(v, \Delta v) = s_0 + vT + \frac{v \times \Delta v}{2\sqrt{a_m b}} \quad (3.2.1.2)$$

where a indicates the acceleration rate; a_m is the maximum acceleration rate; v denotes the current speed; v_d indicates the desired speed (assumed equal to the speed limit in this research); Δv represents the speed difference between the subject vehicle and its preceding vehicle; $\propto$ means the acceleration exponent, which is set as 4 in this research; s is the current headway between the subject vehicle and its preceding vehicle; $s^*(v, \Delta v)$ represents the minimum desired headway; s_0 denotes the standing distances (2.5m); T represents the desired headway (1s); and b is the desired deceleration rate.

3.2.2 W99 Model

W99 is a micro-simulation psychophysical model which has ten parameters available for calibration. These ten parameters are intuitively consistent with human driver behaviors with certain randomness (Durrani et al., 2016). To ensure that the W99 can represent the local traffic accurately, the ten parameters were calibrated to ensure that the average speeds on each approach in the simulation are matched with the ones that were from the field survey according to Hummer (2010).

Considering the data availability, this research selects the minimal difference between simulated average speeds and observed average speed for each approach as the

objective function used in the calibration process. An overall difference within 15% is regarded as acceptable performance.

$$\frac{\left(\sum_i^N \frac{\left|v_{o,i} * -v_{s,i}\right|}{v_{o,i}}\right)}{N} \tag{3.2.2.1}$$

where $v_{o,i}$ and $v_{s,i}$ are the observed and simulated average speed for approach i respectively, and N indicates the total number of approaches.

Genetic algorithm is utilized to minimize the difference between the observed average speeds and simulated average speeds for each approach. GA is a popular and efficient approach in calibrating the car-following model parameters. For brevity, this research skips the introduction of GA, and readers may refer to existing studies of GA calibration for more details (Ma and Abdulhai, 2002). The population size and the maximum number of generations are set as 10 and 20 respectively. The final difference becomes stable at 11%, which is recognized as an acceptable difference (Manjunatha et al., 2013). The obtained parameter values from GA are presented in Table 3.1. The lane changing movement is controlled by the default car-following model in SUMO, i.e., LC2013 (Erdmann, 2015).

TABLE 3.1: GA Calibrated W99 Parameter Values

Parameters	Interpretation	Default Values	Calibrated Values	Value Range
CC0	average standstill distance (meter)	1.4	1.287251	[0.1, 10.0]
CC1	headway (seconds)	1.2	1.569918	[0.1, 5.0]
CC2	longitudinal oscillation (meters)	8	1.28187	[0.1, 15.0]
CC3	start of deceleration process (seconds)	-12	-12.3849	[-27.0, -5.0]
CC4	negative following threshold Δv(m/s)	-1.5	-2.398	[-5.0, 0.0]
CC5	positive following threshold Δv(m/s)	2.1	0.324976	[0.0, 5.0]
CC6	speed dependency of oscillation (10^{-4} rad/s)	6	4.047425	[0.1, 11.0]
CC7	oscillation acceleration - m/s^2	0.25	0.29111	[0.0, 7.0]
CC8	acceleration rate when starting (m/s2)	2	4.582238	[0.1, 7.0]
CC9	acceleration behavior at 80 km/h (m/s^2)	1.5	4.261776	[0.1, 8.0]

3.3 Platooning Control

Vehicle platooning is one of the advanced features of CAVs. It can only be achieved with CAVs that have communication capabilities with other vehicles. Two assumptions were often made with CAVs platooning. One is shorter headways for vehicles inside a defined platoon, and the other is homogenous speeds. With shorter headways and homogenous speeds, the vehicles inside the same platoon can be regarded

as a single unity to travel on the road, which can increase the capacity of the roads and also reduce the computational complexity when trajectory planning is involved. This research has also adopted these concepts to fully release the potentiality of CAVs. Two sets of platooning controls are defined in this research, namely platooning control I and platooning control II. The essential difference between platooning control I and platooning control II lies in that Platooning control II allows CAVs to dynamically adjust their distances to the preceding vehicles.

3.3.1 Platoon Formulation and Splitting

The platoon control system in this research iterates all active vehicles in the simulation environment and checks whether the neighboring vehicles meet the requirements for the platoon formulation. The requirements are that the vehicles:

1) are in the same lane;
2) stay within the range of a certain distance; and
3) share the same path.

If the requirements above are met, then the system can define such a group of vehicles as a platoon and thus share the same speed with the leading vehicle. However, if any of the vehicles inside the platoon fail to suffice these requirements, then the platoon splits up and switches back to the default car-following model.

There is one more condition guaranteeing platoon splitting. When the platoon is approaching an intersection, the remaining green time g_p may not be sufficient for all vehicles in a platoon to pass the intersection together, especially when the platoon size is large. Thus, to make the platoon system practical, the vehicles with platooning are assumed to have the knowledge of remaining green time. With the information on the remaining green time g_p, the platooning system checks whether all vehicles inside a platoon can pass the intersection or not through Equation (3.2.1.1),

$$g_p^w \geq \frac{D_t^i}{v_t^i}, i \in \boldsymbol{P} \tag{3.3.1.1}$$

where g_p^w denotes the remaining green time for the platoon $\boldsymbol{P}$, D_t^i and v_t^i indicate the remaining distance towards the intersection and the speed of the i^{th} vehicle inside the platoon $\boldsymbol{P}$ at the time step t. In the platoon $\boldsymbol{P}$, when the i^{th} the vehicle cannot pass the intersection and the vehicle directly ahead of the i^{th} vehicle, i.e., $i-1^{th}$, can pass the intersection, then the platoon $\boldsymbol{P}$ disbands from the $i-1^{th}$ vehicle. The vehicles after the $i-1^{th}$ vehicle in the platoon $\boldsymbol{P}$ would reform a platoon to decelerate together. When the platoons are approaching the intersection, the platooning system checks Equation (3.3.1.1) for each vehicle in the platoons at every time step. In this manner, the platoon system can avoid the situations where the platoon runs a red light because of its large platoon size.

3.3.2 Platooning Control I

The vehicles inside a platoon share the same speed and keep a constant close distance in between. The platoon speed is naturally determined by the leading vehicle's speed. The platoon attempts to set the following vehicles' speeds the same as that of the leading vehicle within acceleration capacity in every time step. If the speed difference between the leading vehicle and the following vehicle exceeds the acceleration/deceleration capacity, the speeds of the following vehicles will execute the boundary speeds to match the leading vehicle's speed as close as possible, as shown in Equation 3.3.2.1.

$$v_t^{following} = \begin{cases} \max\left(v_{t-1}^{following} - a_L, v_{t-1}^{leading}\right), if\ v_{leading} \le v_{following} \\ \min\left(v_{t-1}^{following} + a_U, v_{t-1}^{leading}\right), if\ v_{leading} > v_{following} \end{cases} \quad (3.3.2.1)$$

where $v_t^{following}$ and $v_{t-1}^{following}$ indicate the speed of the following vehicle at the time step t and time step $t-1$ respectively, and $v_{t-1}^{leading}$ denotes the speed of the leading vehicle at the time step $t-1$.

Indeed, in this system, the distance that guarantees a platoon formulation may have an important influence on the performance of the platooning system. Hence, this research also conducts a sensitivity analysis of this parameter. The selection of distance boundaries ranges from 5m to 31m with an increment of 4m. Each distance boundary has 5 simulation runs and each simulation lasts for 900s (15 minutes). This research obtains the traffic delay and fuel consumptions to determine the optimal searching distance. Figure 3.1 provides the average traffic delay and fuel consumption results for each distance boundary. According to Figure 3.1, it can be observed that both traffic delay and fuel consumption reach the minimum at the distance of 21m, and thus this research selects 21m as the distance boundary for further analyses.

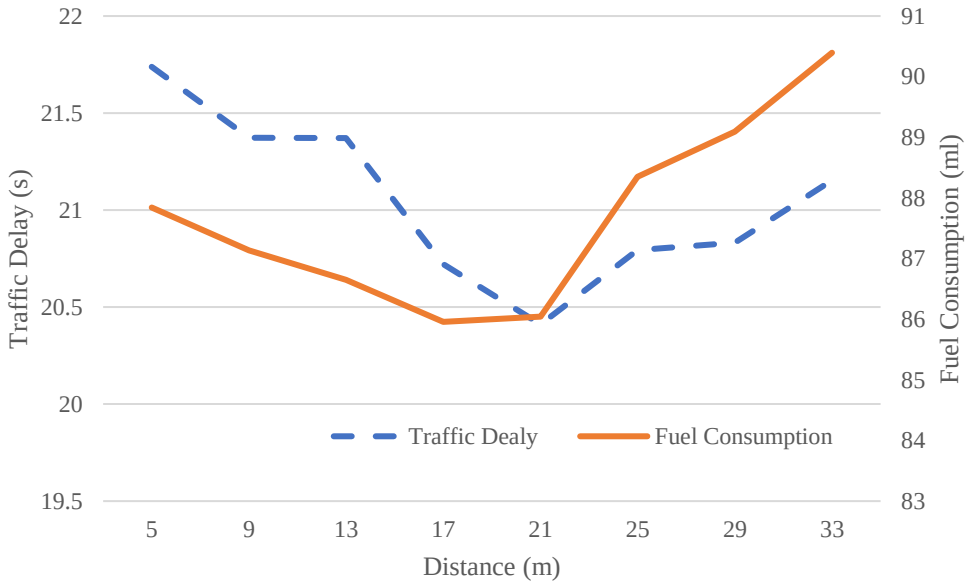

FIGURE 3.1: Performances of platooning with different values of distance boundaries

3.3.3 Platooning Control II

Besides the platooning control introduced in Section 3.3.2, the model developed by Rajamani (2011) is also further incorporated in this research. Based on the literature review, platooning model developed by Rajamani (2011) was one of the most acknowledged platooning models because of tunable parameters and stable performance (Darbha et al., 2017; Darbha et al., 2018; Bian et al., 2019;). Therefore, this research employed such an approach to evaluate the impact of CAV platooning technology in the environment of superstreet. The full form of vehicle platooning model is presented as below,

$$\ddot{x}_d = w_1 * \ddot{x}_{i-1} + w_2 * \ddot{x}_0 + w_3 * \dot{\varepsilon} + w_4 * (\dot{x}_i - \dot{x}_0) + w_5 * \varepsilon_i \quad (3.3.3.1)$$

$$\varepsilon_i = x_i - x_{i-1} + L_{i-1} + g_d \quad (3.3.3.2)$$

$$\dot{\varepsilon}_i = \dot{x}_i - \dot{x}_{i-1} \quad (3.3.3.3)$$

where $\ddot{x}_d$ represents the control input for the subject vehicle in terms of acceleration rates. $\ddot{x}_{i-1}$ and $\ddot{x}_0$ denotes the acceleration rate for the preceding vehicle and the lead vehicle of the platoon. w_1, w_2, w_3, w_4, and w_5 are the control gains for their corresponding terms, such as acceleration of the preceding vehicle $\ddot{x}_{i-1}$. L_{i-1} indicates the vehicle length for the preceding vehicle (all vehicle lengths are assumed to be 5m in later experiments). Figure 3.2 presents the string of vehicles in a platoon.

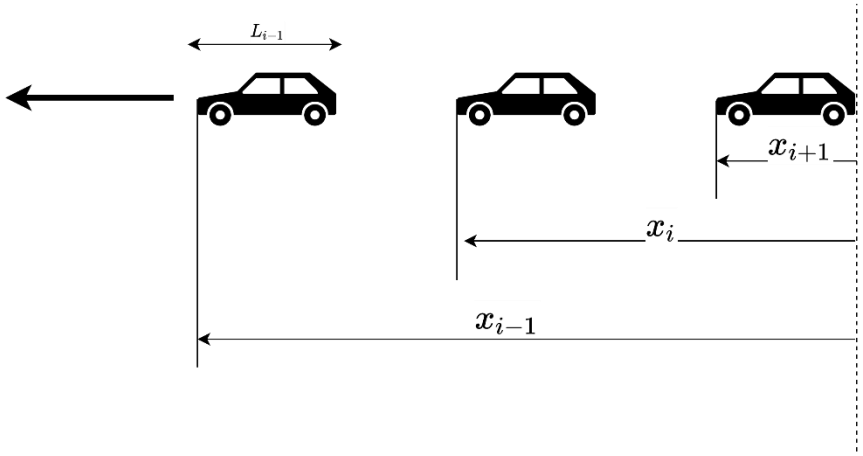

FIGURE 3.2: Sting of vehicles in a platoon

The calculations for five control gains are shown below.

$$w_1 = 1 - C_1 \quad (3.3.3.4)$$

$$w_2 = C_1 \quad (3.3.3.5)$$

$$w_3 = -\left(2 * \xi - C_1 * \left(\xi + \sqrt{\xi^2 - 1}\right)\right) * w_n \quad (3.3.3.6)$$

$$w_4 = -C_1 * \left(\xi + \sqrt{\xi^2 - 1}\right) * w_n \quad (3.3.3.7)$$

$$w_5 = -w_n^2 \quad (3.3.3.8)$$

where C_1 is the weighting factor for the acceleration rates of the leader and the preceding vehicle respectively. ξ is the damping ratio and w_n is the control bandwidth. Among these parameters, C_1, ξ and w_n are tuning parameters that can be adjusted for research needs. Table 3.2 shows the default parameter values that are used in this research. Platoons are only detectable within a certain distance, thus platooning control can only apply to the vehicles that are within a distance boundary D_b. According to (Segata et al., 2014), 20 m is a proper boundary for platooning control. Table 3.2 shows a summary of the values utilized in this research for the platooning control.

TABLE 3.2: Default Values for Platooning Control Parameters

Parameters	Default values
Damping ratio $\boldsymbol{\xi}$	1
Bandwidth $\boldsymbol{w_n}$	0.2 Hz
Acceleration weighting factor $\boldsymbol{C_1}$	0.5
Desired gap $\boldsymbol{g_d}$	5 m
Distance boundary for platooning $\boldsymbol{D_b}$	20 m

A small numerical simulation was conducted to test the effectiveness of platooning model given the default values. Assume a preceding vehicle and a leader vehicle with a speed of $20\ m/s$ and acceleration of $0\ m/s^2$. A third following vehicle is initiated with a speed of $15\ m/s$ and a gap to the preceding vehicle of $20\ m$. Figure 3.3 shows how the vehicle catches up with the platoon of two vehicles using this platooning control system. From Figure 3.3, one can see the platooning control can reduce gap error ε from 15m to 0m in about 30s. Moreover, platooning control system could maintain the desired gap size throughout the whole trip. This result validates the platooning control system in this research.

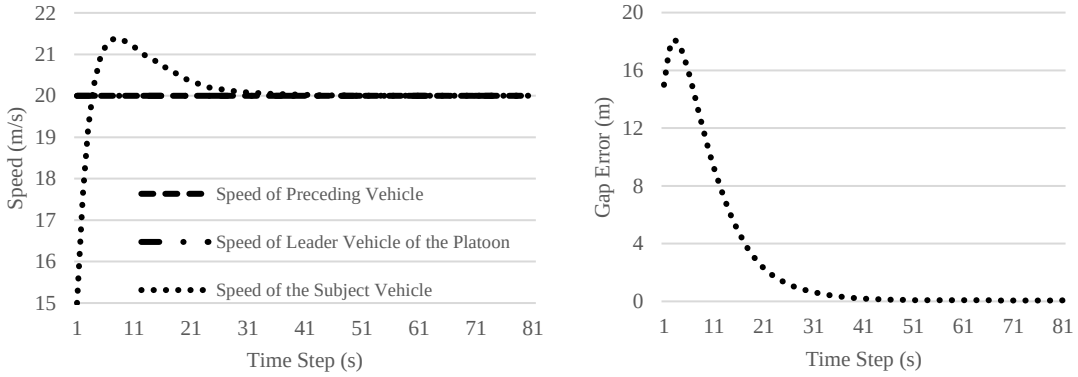

FIGURE 3.3: Numerical test for platooning model performance

Some other practical considerations need to be added in a large-scale microscopic simulation in this research. First, the vehicles can enter a platoon only when they share

the same next route, which means that if the platoon is going to turn left in the upcoming intersection, then only the vehicles that also turn left are allowed to join the platoon and keep a close following distance. Second, the vehicles can enter a platoon only when they share the same lane. If the vehicle inside the platoon violates these two rules at a certain time step, then the platoon will disband, and the rest of the vehicles may reformulate a platoon if they meet the above requirements.

CAVs should also be controlled by the default car following model when CAVs are approaching the signalized intersection. CAVs controlled by platooning mode illustrated by Eq (3.3.3.1-3.3.3.8) result in a slow approaching rate to stopped preceding vehicles, which are often seen in closely spaced signalized intersections such as superstreet. Figure 3.4 illustrates the motivation for this consideration assuming that two CAVs with two different controls are approaching a stopped vehicle at a distance of 100m at the intersection. CAVs controlled by IDM reaches the converged distance (IDM default desired gap 2.5m) in $20s$ while it takes $30s$ for the platooning control to reach the desired distance (platoon default desired gap 5m). If a CAV with platooning control approaches the waiting vehicles in front of intersections in a medium/high traffic volume scenario, this CAV will inevitably block other vehicles in the middle of the road. This prevents us from applying the same platooning control logic throughout the simulation.

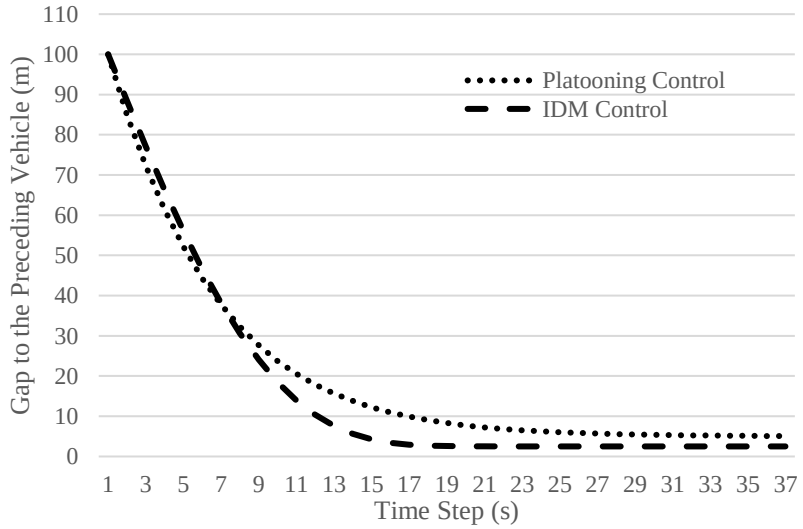

FIGURE 3.4: Gap plot for CAV approaching a stopped vehicle with platooning control and IDM control

Based on the above discussions, the CAVs approaching the signalized intersection in the same lane, are bunched together (when their inter distance is less than 1s headway plus minimum gap, i.e., 2.5m) by sharing the same speed as their platoon leaders to pass the intersection. This design can achieve a similar effect as curve matching algorithms proposed in Gong and Du (2018) and trajectory copy in Han et al. (2020). After the CAVs exit the intersection, platoon control starts to take effect to adjust their headways properly. This research also implements the platoon split as introduced in Han et al. (2020) when the green duration is not sufficient for the whole platoon to travel through.

3.4 Trajectory Planning I with Fixed Signal Timing

3.4.1 Optimal Trajectory Based on Accumulated Absolute Acceleration Rates

CAVs can plan their trajectories based on the signal information obtained to achieve a certain objective, such as minimizing fuel consumption or traffic delay. The popular approach is to formulate trajectory planning as an optimal control problem whose objective can be a certain traffic performance measure. When the goal is to minimize fuel consumption or emissions, the objective function often takes a non-linear form and requires non-linear programming to obtain an optimal solution. Significant computational resources may be required in the real world. A substitute approach to achieving the optimal fuel consumption or emissions benefit is to minimize accumulated absolute acceleration rates along the trajectories according to Feng et al. (2018). First, a generalized trajectory planning problem of CAVs can be formulated with the objective of minimizing cost $\boldsymbol{C}$.

$$\min \boldsymbol{C}(a, v) \tag{3.4.1.1}$$

$$\begin{cases} \dot{x}(t) = v(t) \\ \dot{v}(t) = a(t) \end{cases} \tag{3.4.1.2}$$

$$\begin{cases} x(t_0) = 0 \\ v(t_0) = v_0 \end{cases} \tag{3.4.1.3}$$

$$\begin{cases} x(t_f) = D \\ v(t_f) = v_f \end{cases} \tag{3.4.1.4}$$

$$-a_L \le a(t) \le a_{U,} \tag{3.4.1.5}$$

$$0 < v(t) < v_{max} \tag{3.4.1.6}$$

$$t_0 \le t \le t_f \; and \; t_f \text{ fixed} \tag{3.4.1.7}$$

where $\boldsymbol{C}(a, v)$ represents the cost function, $x(t)$ and $v(t)$ are control variables that indicate the traveled distance and instant speed value at the time step t respectively. $a(t)$ is the control variable that represents the acceleration rate at time step t. t_0 and t_f are the time steps when the CAVs start and finish the trajectory respectively. D is the target distance that the subject vehicle needs to travel, which often is the distance between the vehicle and the intersection. The fuel consumption or emission is known to be significantly related to the acceleration rates. Feng et al. (2018) developed a trajectory planning strategy to minimize fuel consumption based on Pontryagin's Minimum Principle (PMP). Through analysis of PMP, a generalized solution can be achieved with the objective of minimizing the accumulated absolute acceleration rates along the trajectory, which is

$$\min \boldsymbol{C} = \int_{t_0}^{t_f} |a(t)| dt \tag{3.4.1.8}$$

The solution to the optimal trajectory generally results in a three-segment trajectory, in which vehicles remain at a constant speed at the second segment. The first and the third segment have a constant either maximum acceleration or deceleration rate according to the relationship between the initial speed or final speed, as Figure 3.5a

shows. Figure 3.5b provides an example comparison of when CAVs are enabled with and without such trajectory planning feature.

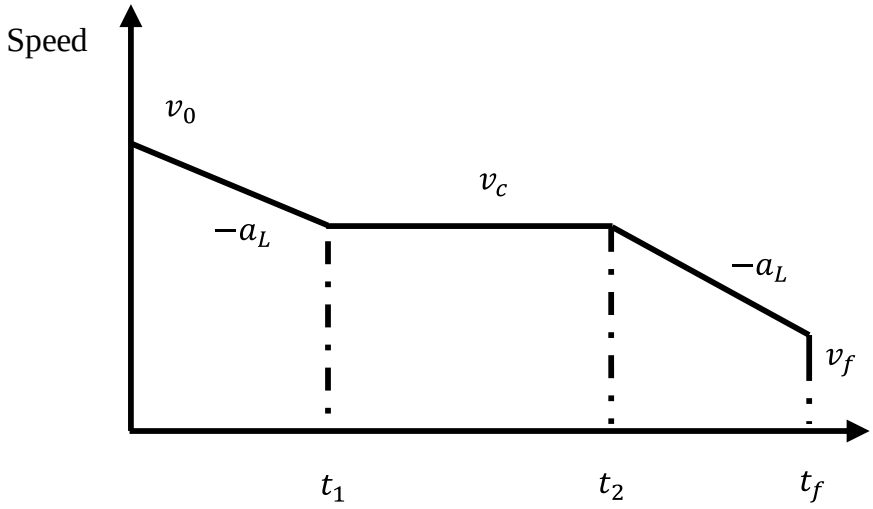

a. Theoretical three-segment trajectory in deceleration case (revised from Feng et al. (2018)

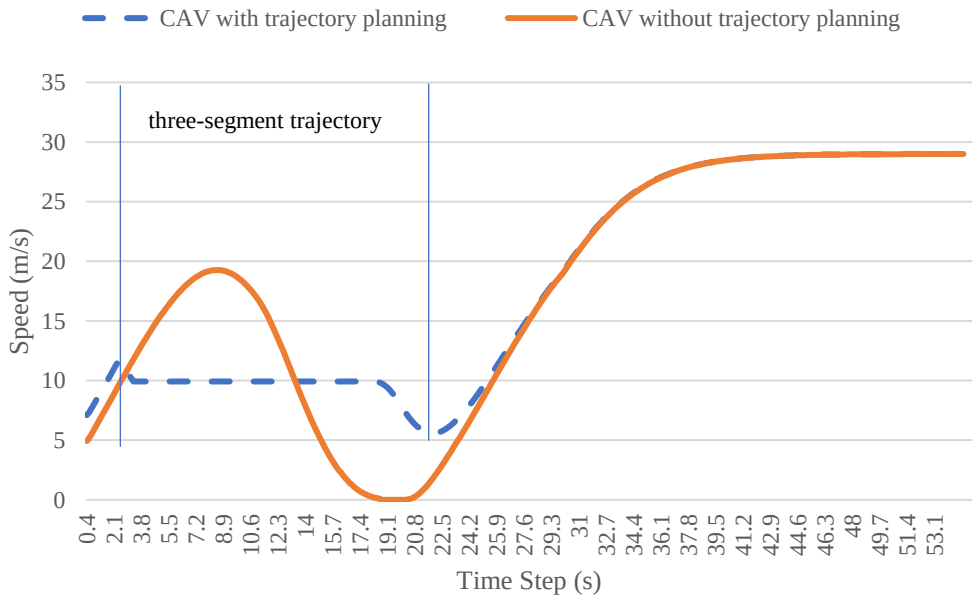

a. Three-segment trajectory in simulation

FIGURE 3.5: A general optimal trajectory for the deceleration scenario

The transition time steps t_1 and t_2 can be determined given the following equations in the deceleration case ($v_0 > v_f$) and acceleration case ($v_0 < v_f$) respectively.

$$\frac{v_0 + v_c}{2} * t_1 + v_c * (t_2 - t_1) + \frac{v_f + v_c}{2} * (t_f - t_2) = D \qquad (3.4.1.9)$$

$$v_c = \begin{cases} v_0 - a_L * t_1 = v_f + a_L\left(t_f - t_2\right), & v_0 > v_f \\ v_0 + a_U * t_1 = v_f - a_U\left(t_f - t_2\right), & v_0 < v_f \end{cases} \quad (3.4.1.10)$$

Additionally, one can obtain the lower and upper travel time boundary to guarantee that a feasible solution exists as shown below:

$$v_0 > v_f \begin{cases} t_L = \dfrac{D}{v_0} + \dfrac{\left(v_0 - v_f\right)^2}{2 * v_0 * a_L} \\ t_U = \dfrac{D}{v_f} - \dfrac{\left(v_0 - v_f\right)^2}{2 * v_f * a_L} \end{cases} \quad (3.4.1.11)$$

$$v_0 < v_f \begin{cases} t_L = \dfrac{D}{v_f} + \dfrac{\left(v_0 - v_f\right)^2}{2 * v_f * a_U} \\ t_U = \dfrac{D}{v_0} - \dfrac{\left(v_0 - v_f\right)^2}{2 * v_0 * a_U} \end{cases} \quad (3.4.1.12)$$

Notably, a feasible three-segment trajectory solution only exists when the vehicle arrival time t_f is strictly within the boundary of t_L and t_U, i.e.,

$$t_L < t_f < t_U \quad (3.4.1.13)$$

When $t_f = t_L$ or $t_f = t_U$, the three-segment trajectory solution collapses into the two-segment trajectory. The lower/upper-time boundaries indicate two-segment trajectories in acceleration and deceleration respectively as shown in Figure 3.6. In a deceleration scenario, the lower boundary indicates that the vehicle keeps its current speed in the first segment and then decelerates to its final speed in the second segment. The upper boundary indicates that the vehicle first decelerates to the target final speed, and then keeps the target final speed until it arrives at the intersection. On the other hand, in an acceleration scenario, the lower boundary indicates that the vehicle first accelerates the final speed v_f and then cruises at the target speed until arriving at the intersection. When the final speed v_f is equal to the maximum speed v_{max}, such trajectory type can yield the minimum travel time $t_{minimum}$ and thus is referred to as the minimum travel time trajectory. The upper boundary in an acceleration scenario means that the vehicle first keeps its initial speed and then accelerates to its target speed. Intuitively, when the travel time is strictly within the lower- and upper-time boundaries, then an optimal three-segment trajectory exists. When the travel time is equal to one of the two boundary values, a two-segment trajectory introduced above can be applied. Nevertheless, when travel time exceeds the boundary, no feasible solution exists with the given distance, acceleration rate, and initial speeds. This reflects the real-world scenarios. For example, a vehicle may not be able to decelerate to a speed of zero if the remaining distance to the intersection is too short or the initial speed is too high.

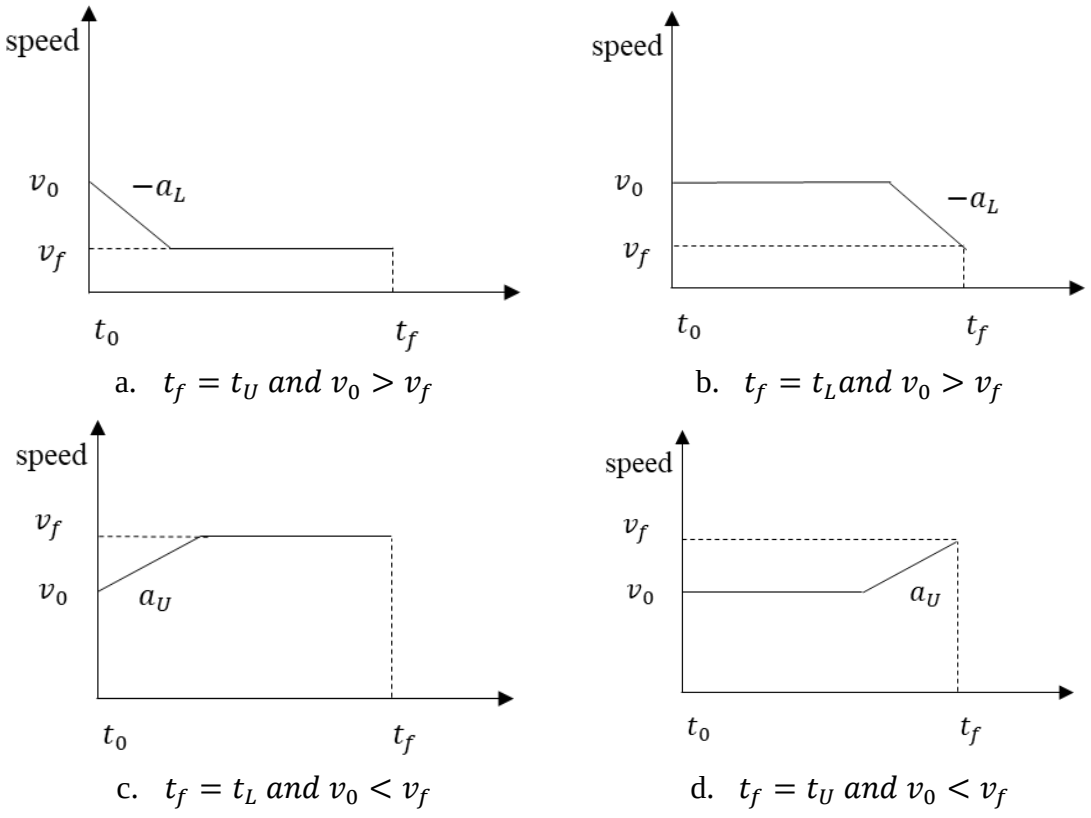

FIGURE 3.6: Two-segment trajectory when t_f equals to boundary values ($t_L \; and \; t_U$)

Feng et al. (2018) demonstrated that this trajectory planning strategy could successfully reduce traffic delay and fuel consumption in a standard isolated conventional intersection with a joint adaptive signal optimization algorithm. With the adaptive signal control, Equation 3.4.1.13 holds for most cases and the vehicle can avoid stops under certain traffic conditions. Nevertheless, this strategy cannot be directly transferred to a fixed signal-controlled intersection. In a fixed signal-controlled intersection, the final travel time t_f is largely dependent on the initiation time or remaining time of the target green phase in a fixed signal timing plan, where vehicles cannot avoid stopping entirely. To apply this trajectory planning scheme in a fixed signal-controlled intersection, this research also considers a constant deceleration trajectory when Equation 3.4.1.13 cannot be sufficient. For a constant deceleration trajectory, the vehicle will keep a constant deceleration rate until it arrives at the intersection with a speed of 0, as shown in Figure 3.7. The deceleration rate a_{dec} can be easily obtained through the basic kinetic law, which is described by Equation 3.4.1.14.

$$a_{dec} = \frac{v_0}{\frac{2 * D}{v_0}} \tag{3.4.1.14}$$

Based on the signal status and the next signal switch time t_{switch}, the vehicle can choose different speed trajectories as introduced above.

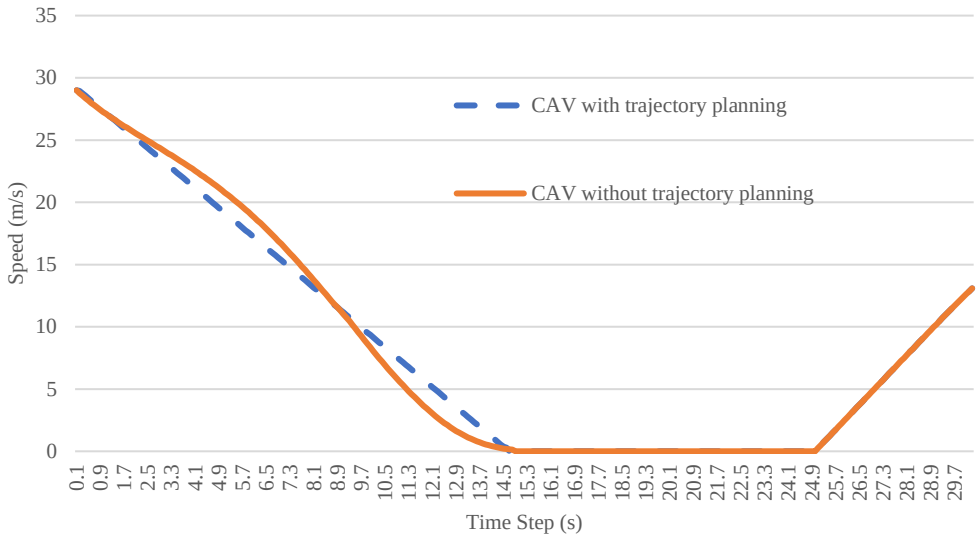

FIGURE 3.7: Constant deceleration trajectory

3.4.2 Trajectory Planning at the Red Signal

When the upcoming signal status for the subject vehicle is red, the signal switch time t_{switch} indicates the initiation of green time. The lower time boundary obtained through Equation 3.4.1.12 is equal to the minimum travel time $t_{minimum}$ when the given final speed $v_f = v_{max}$. If the switch time t_{switch} is less than or equal to the $t_{minimum}$, then the vehicle can meet a green signal with a two-segment trajectory as shown in Figure 3.8 to achieve minimal traffic delay.

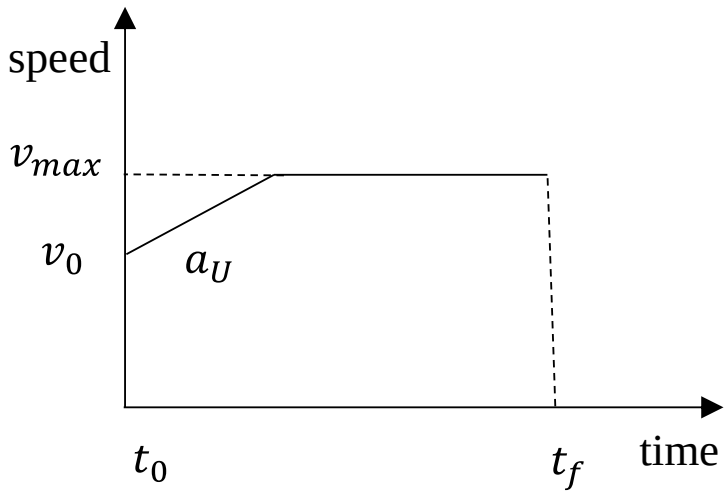

FIGURE 3.8: Speed trajectory with minimum travel time

If the switch time is greater than the minimum travel time, i.e., $t_{switch} \geq t_{minimum}$, then the vehicle with a minimum travel time trajectory will meet a red signal. In this situation, it is assumed that $t_f = t_{switch}$. From Equation 3.4.1.11 and Equation

3.4.1.12, one may obtain $t_L$and t_U given a final speed v_f. Hence, researchers may simply enumerate all possible final speeds $[0, v_{max})$ to obtain feasible speed candidates $\boldsymbol{V_f}$ so that Equation 3.4.2.1 stands.

$$t_L < t_{switch} < t_U \tag{3.4.2.1}$$

This research selects the max($\boldsymbol{V_f}$) so that the subject vehicle can travel through the intersection with maximum final speed to minimize the traffic delay, where the max() function returns the maximum value among the feasible final speed list $\boldsymbol{V_f}$.

3.4.3 Trajectory Planning at Green Signal

If the ahead signal status is green, then $t_{signal\ switch}$ indicates the remaining green time for the subject vehicle. This research mainly considers two cases based on the relationship between signal switch time $t_{signal\ switch}$ and minimum travel time $t_{minimum}$ of the subject vehicle.

Case 1: when the subject vehicle can traverse through the intersection with minimum travel time $t_{minimum}$ (i.e., $t_{signal\ switch} \geq t_{minimum}$), then the vehicle may accelerate its maximum speed to pass the intersection to achieve the minimal traffic delay. However, this strategy may potentially increase the average fuel consumption as the fuel consumption is closely related to the acceleration rate. In some circumstances, if the $t_{signal\ switch} \geq t_{current\ speed}$, where $t_{current\ speed}$ is the travel time to the intersection when the vehicle keeps its current speed, then the decision-makers who assign a higher priority on fuel consumption may let the vehicle keep its current speed to avoid increasing fuel consumption with acceptable compromise on the traffic delay.

Case 2: $t_{signal\ switch} \leq t_{minimum}$ means the subject vehicle cannot arrive at the intersection with the given remaining green time even if the vehicle accelerates to maximum speed. In such a situation, a constant deceleration trajectory introduced above may be executed. The subject vehicle may need to check whether the vehicle can meet the second green with a given final speed within $[0\ v_{max})$ when the distance D is large.

3.4.4 Encountering Preceding Vehicles during Trajectory Planning

In the real world, the vehicles may be close to preceding vehicles on the road, and following the predetermined trajectories may lead to collisions with the preceding vehicles. Therefore, to avoid these collisions in this research, when a vehicle has preceding vehicles that are within a $3s$ headway, the vehicle will stop executing the planned trajectory and switch to the predefined car-following model, which is the IDM in this research. Note that the system constantly checks each vehicle's distance to the preceding vehicles at each time step. When the distance to the preceding vehicle is greater than $3s$ and there is an upcoming signalized intersection, then the system will plan the vehicle trajectory again for the subject vehicle to follow. With this function, the vehicles following the planned trajectory can successfully avoid collision with not only

the close preceding vehicles but also the queueing vehicles in front of the intersection because of the red signal.

3.5 Adaptive Signal Control

This research conducts preliminary research on the potential impact of adaptive signal control to leverage the communication between CAVs and signalized intersection. The adaptive signal control in this research can update its phasing duration and phase sequence according to the arrival information of CAVs.

3.5.1 Signal Optimization with MILP

Adaptive signal control leverages the communication between CAVs and signalized intersection. The adaptive signal control in this research can update its phasing duration and phase sequence according to the arrival information of CAVs.

The adaptive signal control model was developed based on the work of Ding et al. (2021). In Ding et al (2021), mixed-integer quadratic programming (MIQP) was developed for CAV platoons based on the arrival times of platoon leaders and platoon length, i.e., the number of vehicles. The formulation of the MIQP model allows for a flexible phasing sequence with the introduction of Big M and auxiliary binary variables. This research utilizes the flexible phase sequence concept in the following mixed-integer linear programming (MILP) formulation. Table 3.3 illustrates the symbols that are used in the following sections.

TABLE 3.3: Descriptions on Symbols Employed in Signal Optimization Modeling

Descriptions	Symbols
Green start	ST
Green duration	G
Vehicle arrival time list	A
Traffic delay	D
Function returning the length of the arrival time list, i.e., the number of vehicles	$N()$
Total number of phases	P
Cycle length	C
Number of lanes	Ln
Average headway	h
Green duration set required by movements	G_M
Minimum clearance interval	c

The delay for vehicle i with a target phase p is defined as the time differences between the green start time ST_p and vehicle arrival time $A_{i,p}$, where $p \in P$ and $i \in A_p$

$$D_{i,p} = \begin{cases} ST_p - A_{i,p}\,; & if\ ST_p - A_{i,p} \geq 0, \\ 0; & if\ ST_p - A_{i,p} < 0 \end{cases} \quad (3.5.1.1)$$

The arrival time of vehicle i can be estimated by the remaining distance l_i divided by the current speed $v_{current,i}$

$$A_{i,p} = \frac{l_i}{v_{current,i}} \quad (3.5.1.2)$$

Naturally, the objective function can be identified as the total accumulated delay from all the vehicles and all phases in the intersection at the current time step, i.e.,

$$\min \sum_{p \in P} \sum_{i \in A_p} D_{i,p} \quad (3.5.1.3)$$

where P is the total number of phases for the target intersection. Two crucial parameters in signal control logic are phase sequences and phase duration. Phase duration G_p can be easily determined based on traffic demand from all the movements belonging to phase p. Assuming traffic movement m is governed by phase p, the green duration required by movement m can be calculated as

$$G_m = \frac{N(A_m)}{Ln_m} * h, \qquad m \in p \quad (3.5.1.4)$$

where G_m denotes the green duration required by the movement m and A_m contains the vehicle arrival times for movement m that has the target phase p. N denotes the function that returns the length of the arrival time list, i.e. number of the vehicles. Ln_m represents the number of lanes available for movement m. Let $G_{M,p}$ contain the green duration set required by each movement from phase p, then the green duration for phase p should suffice the critical traffic movement volume for phase p, i.e.,

$$G_p \geq \max(G_{M,p}) \quad (3.5.1.5)$$

Different phase sequences may cause significant performance changes in the traffic operations. Hence, this research utilizes the binary earlier indicator Ω. For a pair of conflicting phases, p and $\neg p$, one can have constraints as shown below,

$$\Omega_{p,\neg p} + \Omega_{\neg p,p} = 1 \quad (3.5.1.6)$$

Specifically, $\Omega_{p,\neg p}$ equals to 1 when phase p turns green in advance of phase $\neg p$, which is the conflicting phase for phase p. In contrast, $\Omega_{p,\neg p}$ equals to zero when phase p turns green after its conflicting phase $\neg p$ turns green.

This research employs the formulation proposed by Ding et al. (2021) to enforce the constraint that conflicting phases do not start simultaneously. In addition, the time difference between conflicting phases should also take into account the minimum clearance time. Therefore, one can have the constraints as follows,

$$ST_p + M * \Omega_{p,\neg p} \geq ST_{\neg p} + G_{\neg p} + c \quad (3.5.1.7)$$

$$ST_{\neg p} + M * \Omega_{\neg p,p} \geq ST_p + G_p + c \quad (3.5.1.8)$$

In this research, it is assumed that the minimum clearance time is 2s. To ensure that the planned signal timing can suffice the vehicle arrivals at the current time step, the sum of the green start and green duration should be greater than the latest arrival time, i.e.,

$$ST_p + G_p \geq \max(A_p) + h \quad (3.5.1.9)$$

However, this constraint may cause the green start and green duration to become unexpectedly large, hence, penalties are added towards green duration and green start in the objective function, which results in the final objective function as presented below.

$$\min \sum_{p \in P} \sum_{i \in A_p} D_{i,p} + w_G * \sum_{p \in P} G_p + w_{ST} * \sum_{p \in P} ST_p \quad (3.5.1.10)$$

The w_G and w_{ST} are the penalty weights for the green start and green duration respectively. These two weights need to be less than 1 since the main objective is to minimize the traffic delay. Hence, this research selects 0.1 for these two weight values. Since the sum of the weights needs to be equal to 1, this leaves the weight for traffic delay w_d as 0.8. To sum up, the full form of the MILP model for signal optimization is presented below:

$$\min \ w_d \sum_{p \in P} \sum_{i \in A_p} D_{i,p} + w_G * \sum_{p \in P} G_p + w_{ST} * \sum_{p \in P} ST_p \quad (3.5.1.11)$$

$$Constraints: D_{i,p} = \max(ST_p - A_{i,p}, 0)$$

$$A_{i,p} = \frac{l_i}{v_{current,i}}$$

$$G_p \geq \max(G_M)$$

$$ST_p + G_p \geq \max(A_p) + h$$

$$\Omega_{p,\neg p} + \Omega_{\neg p,p} = 1$$

$$ST_p + M * \Omega_{p,\neg p} \geq ST_{\neg p} + G_{\neg p} + c$$

$$ST_{\neg p} + M * \Omega_{\neg p,p} \geq ST_p + G_p + c$$

The above optimization model has a MILP form that is convenient for popular commercial solvers to solve, such as CPLEX or Gurobi. This research uses Gurobi to obtain the solution in real-time.

3.5.2 Additional Practical Considerations for Adaptive Signal Control

Rolling Horizon Scheme

Since vehicle arrivals vary at different periods at the microscopic level, it is often necessary to utilize a rolling horizon scheme to update the vehicle arrival information and

signal timings. In this research, the vehicle arrival information and signal timing are updated as soon as all vehicles in the previous cycle finished traveling through the intersection. This rolling horizon scheme is also illustrated in Figure 3.9, where C_n denotes the cycle length for the n^{th} cycle. The initial time for each cycle is reset as zero.

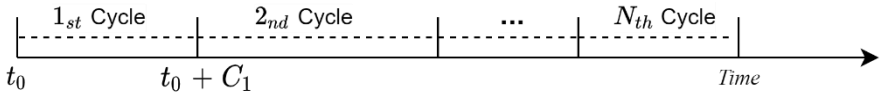

FIGURE 3.9: Rolling horizon scheme illustration

Filling up Cycle in Low Traffic Volume Scenarios

Although the proposed signal optimization model can continuously yield the optimal signal timings for vehicle arrivals in time step t, there are some extreme traffic scenarios that deserve attentions. In low traffic volumes, there may be no traffic for a considerable time periods for a particular approach, and the designed signal optimization scheme may produce frequent but unnecessary signal switches between conflicting phases. Though these unnecessary signal switches do not compromise the traffic delay, they may cause confusions to other road users and extra wear for the signal displaying equipment in real-world deployment. Therefore, when all detected vehicles belong to one phase in an intersection at time step t, the targe phase fills up all planned cycle length. Figure 3.10 illustrates this filling up cycle process.

	Vehicle Arrivals (1 vehicle arrival; 0 no vehicle arrival)				Optimized Signal Timing (1 green; 0 red)			Filled up Signal Plan (1 green; 0 red)	
Cycle	Time Step	p_1	p_2	Signal Optimization →	p_1	p_2	Filling Up Cycle →	p_1	p_2
	1	0	0		0	0		0	1
	2	0	0		0	0		0	1
	3	0	0		0	0		0	1
	4	0	0		0	0		0	1
	5	0	1		0	1		0	1
	6	0	1		0	1		0	1
	7	0	1		0	1		0	1

FIGURE 3.10: Filling up cycle procedure

Emergency Release in High Traffic Volume Scenarios

In extreme high traffic volume scenarios, the minimal-traffic-delay oriented signal timing plan may cause vehicles from minor approaches to wait excess long periods.

When vehicles have waited for two standard cycle lengths ($120s \times 2$ for this research) in front of the intersection, the signal should turn green for a sufficient duration ($3s$) so that the vehicle can pass the intersection. This operation also reflects the equity principle in traffic operations. Figure 3.11 presents the overall workflow for this adaptive signal control.

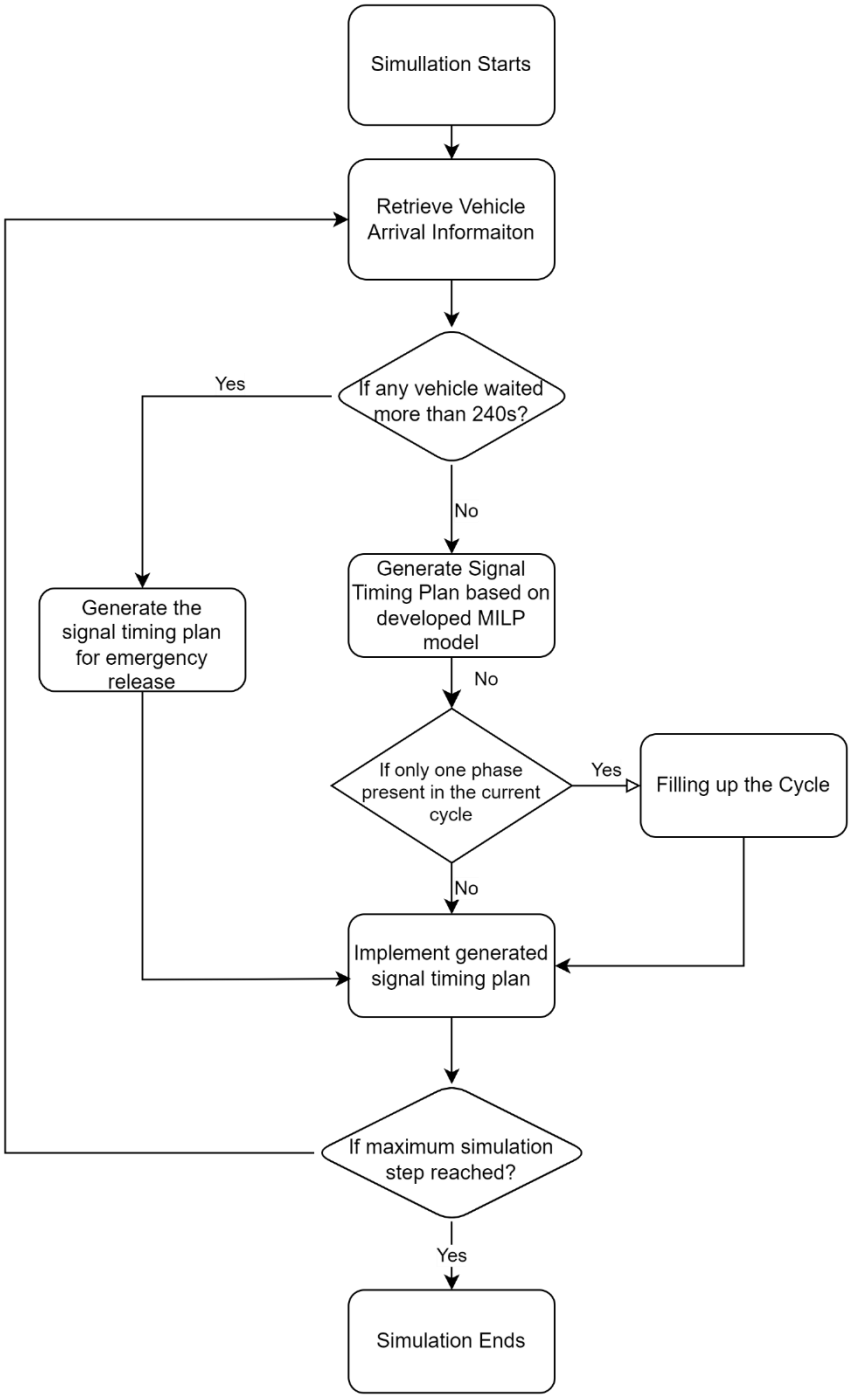

FIGURE 3.11: Overall flow chart for optimized signal timing procedures

3.5.3 Trajectory Planning with Adaptive Signal Control

For the trajectory planning under adaptive signal control, this research employs the Ding et al. (2021) model to explore the impact of CAVs. Ding et al. (2021) developed the trajectory planning based on the work of Feng et al. (2018), in which three-segment trajectory planning was proven to be an efficient approach to reducing traffic delay while preventing that fuel consumption increases. To avoid unstable traffic flow, Ding et al. (2021) further simplified this approach by only considering three-segment acceleration trajectories (two segment trajectory is a special case of three-segment trajectory when the green start time is equal to the boundary value, refer to Feng et al. (2018) and Ding et al. (2021) for more details). The discussion on trajectory planning varies based on the relationship between the earliest arrival time of vehicle i and the optimized green start ST_p. The earliest travel time i_p^e is when the vehicle accelerates with the maximum acceleration rate until it reaches the speed limit, it travels through the intersection with the speed limit. Equation (3.5.3.1) shows the calculation of i_p^e.

$$i_p^e = \begin{cases} \dfrac{\sqrt{\left(v_{curent,i,p}\right)^2 + 2a^U l_{i,p}} - v_{current,i,p}}{a^U}, & l_{i,p} < \dfrac{v_f^2 - v_{current,i,p}^2}{2a^U} \\ (l_{i,p} - \dfrac{v_f^2 - v_{current,i,p}^2}{2a^U})/v_f + \dfrac{v_f - v_{current,i,p}}{a^U}, & l_{i,p} \geq \dfrac{v_f^2 - v_{current,i,p}^2}{2a^U} \end{cases} \quad (3.5.3.1)$$

Case 1: $ST_p \leq i_p^e$

When the green start time for phase p is less than the earliest arrival time of vehicle i, i_p^e, the vehicle can meet a green signal with its fastest speeds, v_f. In such case, the vehicle may accelerate from its current speed $v_{current,i,p}$ with its maximum acceleration capability a^U to the speed limits instantly, and then cruise at its maximum speed to travel through the intersection. The time required to accelerate to v_f can be obtained as follows,

$$t_1 = \frac{\left(v_f - v_{current,i,p}\right)}{a^U} \quad (3.5.3.2)$$

Case 2: $i_p^e \leq ST_p < t_{three,i,p}$

$t_{three,i,p}$ is a boundary value for the vehicle that first travels with current speed, then accelerates with a^U to the speed limit, and keeps driving at the speed limit to travel through the intersection. In this case, the acceleration rate of the subject vehicle experiences three stages, $\{0, a^U, 0\}$. $t_{three,i,p}$ can be obtained as follows:

$$t_{three,i,p} = \frac{l_{i,p}}{v_{current,i,p}} - \frac{\left(v_f - v_{current,i,p}\right)^2}{2 * v_{current,i,p} * a^U} \quad (3.5.3.3)$$

where $l_{i,p}$ denotes the remaining distance to the stop line. The two transition point time points t_1, t_2 for this three-segment trajectory can be calculated as follows:

$$t_1 = \frac{v_f * ST_p - l_{i,p}}{v_f - v_{current,i,p}} - \frac{\left(v_f - v_{current,i,p}\right)}{2 * a^U} \tag{3.5.3.4}$$

$$t_2 = \frac{v_f - v_{current,i,p}}{a^U} \tag{3.5.3.5}$$

Case 3: $ST_p = t_{three,i,p}$

When the boundary value $t_{three,i,p}$ equals to the green initiation time ST_p for the subject vehicle i, the three-segment trajectory collapse into two segments, in which the subject vehicle first keeps its current speed and then accelerates to its maximum allowed speed with a^U. Then the acceleration segments would be $\{0, a^U\}$. The subject vehicle reaches its maximum speed and the stop line simultaneously in this case. The split time t_1 for the two-segment acceleration trajectory can be easily calculated as follows:

$$t_1 = ST_P - \frac{v_f - v_{current,ip}}{a^U} \tag{3.5.3.6}$$

Case 4:$t_{three,i,p} < ST_p < t_{v_{current},i,p}$

$t_{v_{current,i,p}}$ is the time for the subject vehicle i to arrive at the intersection with current speed. When the green start time ST_p falls between $t_{three,i,p}$ and $t_{v_{current},i,p}$, the subject vehicle i can only reach the free speed if there is a deceleration segment. Nevertheless, a deceleration three-segment may cause unstable traffic flow and larger fuel consumption may be incurred. Therefore, to make the trajectory planning efficient and robust, a two-segment control scenario is employed, that is, $\{0,a^U\}$. The subject vehicle needs to keep the current speed long enough so that it can reach a target speed $v_f{}'$ ($v_f' < v_f$) with maximum acceleration capacity. Similar to the discussions above, the calculation of t_1 is given in Equation (3.5.3.7).

$$t_1 = ST_p - \sqrt{2 * \frac{l_{i,p} - v_{current,i,p} * ST_p}{a^U}} \tag{3.5.3.7}$$

This finishes the illustration of the trajectory planning model. Nevertheless, another issue arises when implementing trajectory planning in simulation environments. By following the predetermined trajectories, CAVs may collide with each other when the preceding vehicles slow down, and the following vehicle speeds up to catch the upcoming green signal. Due to this issue, CAVs must stop following the predetermined trajectories when their inter gap is close to a threshold. Through a trial-and-error experiment, this research selects a 1.5s headway gap as such threshold considering both safety and efficiency. This means that CAVs would switch back to default IDM car following mode when their distance has a smaller or equal to 1.5s headway. Also, if i_p^e of

vehicle i is greater than the sum of the green start and green duration of its target phase, then this vehicle cannot meet a green signal in the currently planned cycle. In this case, the subject vehicle will keep moving based on IDM and will not enter the trajectory planning module until the next planned cycle initiates.

3.6 Information on the Selected Location for Case Study

A superstreet situated in Leeland, NC is identified for the case study. This superstreet is selected for its typical geometric design and traffic flow characteristics. The traffic characteristic information on the selected superstreet was available in Hummer et al. (2010). Figure 3.12 shows the selected superstreet and signal locations in Google Maps and Table 3.4 provides the traffic characteristics information. The maximum speed limits are set as 29 m/s (i.e., 65mph) for the main road and 15.6 m/s (i.e., 35mph) for the minor road. The four minor intersections in the superstreet system are all signal-controlled with a cycle length of 120s.

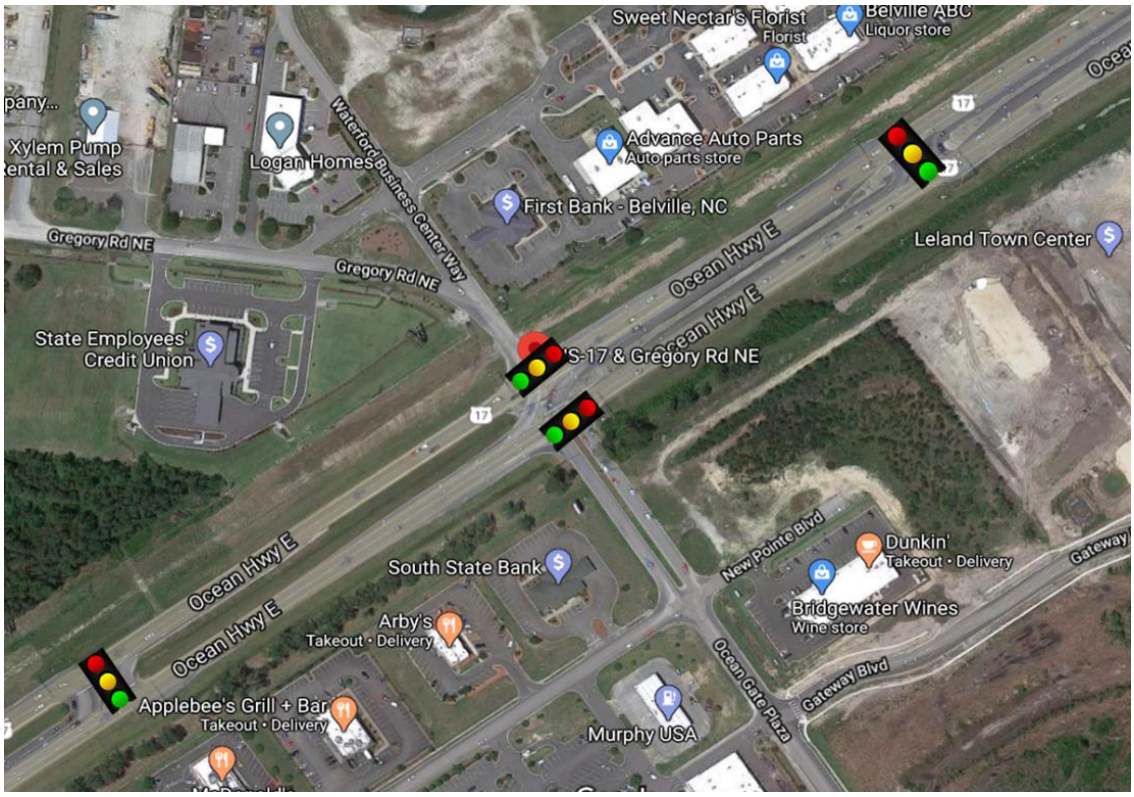

FIGURE 3.12: Selected superstreet for the case study and signal locations (adapted from the screenshot of Google Maps)

TABLE 3.4: Traffic Characteristic Information on the Superstreet at Leeland, NC

Approach	Average speed (m/s)	Peak hour demand	Average stops	Travel time (Minutes)
EBL	5.99	18	3	2.45
EBR	6.93	20	2	1.38
EBT	5.68	9	2	2.25
NBL	8.00	20	1	1.17
NBR	14.08	71	0	0.64
NBT	14.75	2029	0	0.81
SBL	5.72	321	1	1.26
SBR	14.26	38	0	0.4
SBT	19.58	1637	0	0.58
WBL	8.09	66	2	2
WBR	7.69	345	1	0.89
WBT	5.05	11	2	2.09

3.7 Simulation Scenarios and Relevant Settings

An equivalent conventional intersection with the same road segment length, lane configuration, and maximum speed are designed in the simulation platform. The cycle length is also set the same as the superstreet in the real world, i.e., 120s, to make a fair comparison. The green splits for each approach are determined by their volume ratios. To account for different traffic conditions, this research tests four different traffic scales including 25%, 50%, 75%, and 100% of peak hour traffic volumes from Table 3.2. Furthermore, a market penetration analysis is conducted on the 100% peak hour traffic volumes. 25%, 50%, and 75% of CAV market penetration rates are considered in the simulation. Every scenario is run five times with different random seeds to account for the randomness. To make the system more robust and increase calculation accuracy, the simulation resolution is set as 10HZ, which means that the simulation runs 10 time steps every second. Once the vehicle enters the roadway network, the vehicle is assumed to enter the Vehicle-to-Infrastructure (V2I) communication range, which is reasonable since the selected superstreet has a rather short road segment length in all approaches before the traffic signals (less than 300m). Average traffic delay (delay per vehicle) and fuel consumption (fuel consumption per vehicle) are the performance indicators that are used for this research. Traffic delay is measured by the ideal travel time (free-flow speed without any stop) minus actual travel time. Fuel consumption is measured by the default emission model from SUMO, i.e., HBEFT.3 (Krajzewicz et al., 2015). The maximum acceleration rates and deceleration rates for IDM are set as 2.5 m/s^2. Considering drivers' comfort, the maximum acceleration rate and deceleration rate in CAV trajectory planning are 2 m/s^2. The simulation experiment for Section 4.2 and the adaptive signal control in Section 4.3 last for 3600s. The remaining experiments from Section 4.3 last for 1800s to facilitate this research.

CHAPTER 4 RESULTS AND ANALYSIS

4.1 Introduction

This chapter discusses the simulation results from different scenarios defined in Chapter 3. The results and discussions are divided into two parts. The first part focuses on the results of platooning control I and trajectory planning I with fixed signal timing, while the second part presents the platooning control II and adaptive signal control signal timing. The results and discussions cover different traffic scales, different environments, and different performance indicators.

4.2 Platooning Control I and Trajectory Planning Control I at Fixed Signal Timing

4.2.1 The Performance of CAVs in Conventional Intersections

4.2.1.1 Traffic Delay

To provide an initial understanding of the performance of CAVs, this research first obtains the simulation results of CAVs from the equivalent conventional intersection. The traffic delays results are presented in Figure 4.1. From Figure 4.1, it can be observed that the developed platooning, trajectory planning, and platooning-based trajectory planning can reduce the traffic delay in most scenarios. The exception is CAVs with platooning at 25%. When CAVs are enabled with platooning, the speed of the following vehicles is influenced by the leading vehicle in the same platoon and may not be able to achieve their maximum speeds even in the light traffic volume conditions. This may potentially explain that no benefit is gained for platooning in the traffic demand of 25% and 50% peak hour traffic volume scenarios. The traffic delay improvements for CAV with platooning become clearer as the traffic demand increases.

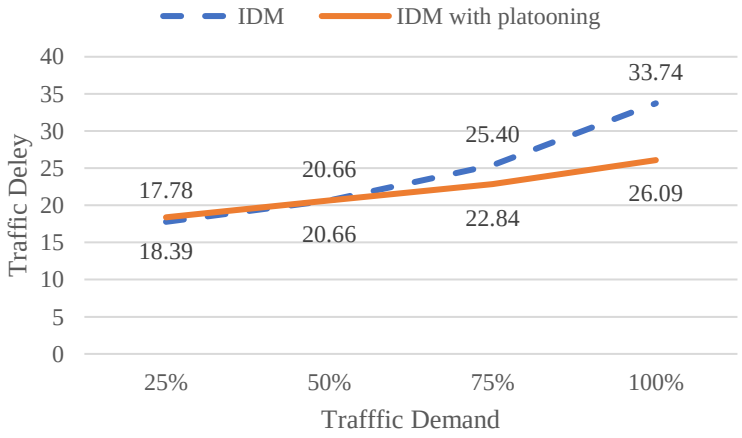

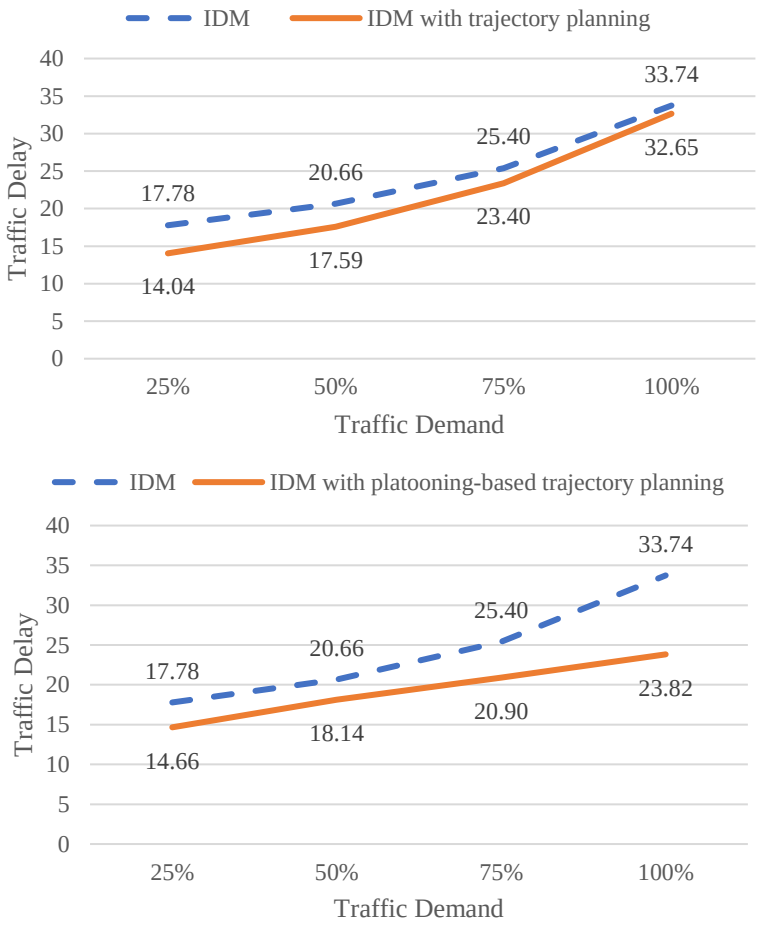

FIGURE 4.1: Average traffic delay(s) of CAVs in the equivalent conventional intersection

Trajectory planning can reduce traffic delay to a larger extent in light traffic volume scenarios, and the improvement magnitudes shrink as the traffic volumes increases. These results can be explained by the trajectory planning modeling framework. As mentioned in the methodology section, to avoid collisions with preceding vehicles and queueing vehicles in front of the intersection, CAVs with trajectory planning may switch to the default car following model frequently in high traffic demand scenarios. For CAV with platooning-based trajectory planning, the traffic delays share a similar trend as the ones from CAV with platooning. Notably, platooning-based trajectory planning also successfully reduces the traffic delay in low traffic demand scenarios.

4.2.1.2 Fuel Consumption

From Figure 4.2, it can be observed that platooning could provide larger benefits in terms of fuel consumption in high traffic volume scenarios. The improvement magnitudes are also consistent with existing studies on platooning (Alam et al., 2015). The proposed trajectory planning framework reduces the average fuel consumption to a certain extent in low traffic volume scenarios. However, the fuel consumption benefits from trajectory planning are less significant compared to platooning. In addition, the trajectory planning framework may produce adverse effects towards fuel consumption in

high traffic volume scenarios, as observed in 100% peak hour traffic volume scenarios. In high traffic volume scenarios, CAVs with trajectory planning capability change to the car following model frequently because of the presence of preceding vehicles, which may produce speed fluctuations and higher fuel consumption. CAV with platooning-based trajectory planning produces the optimal fuel consumption results at most traffic demand levels.

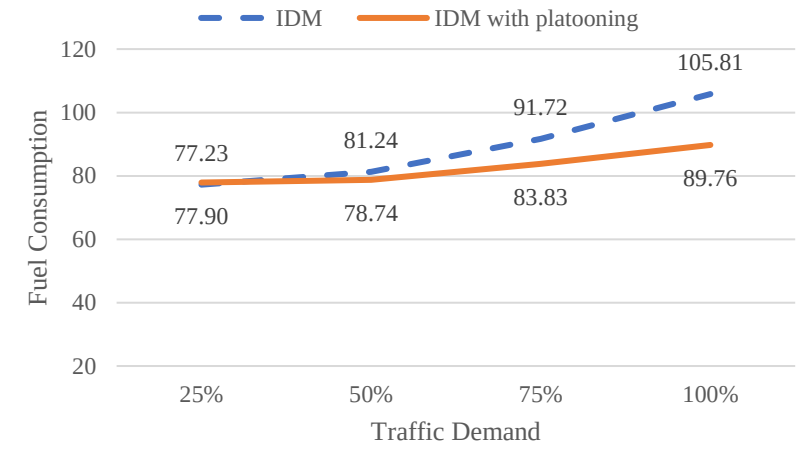

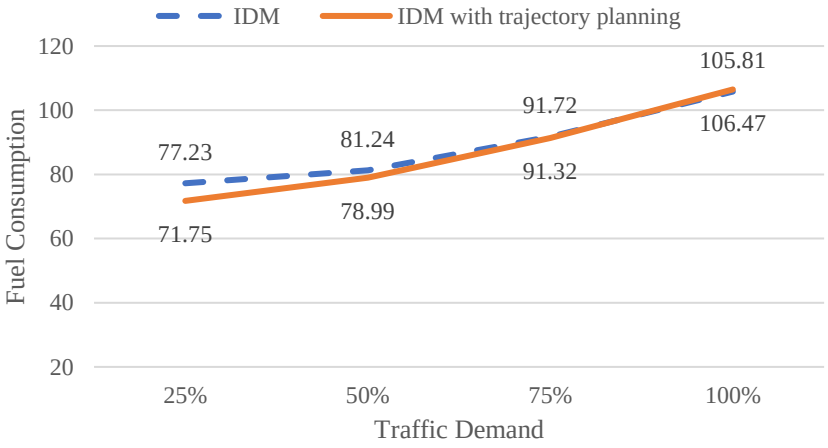

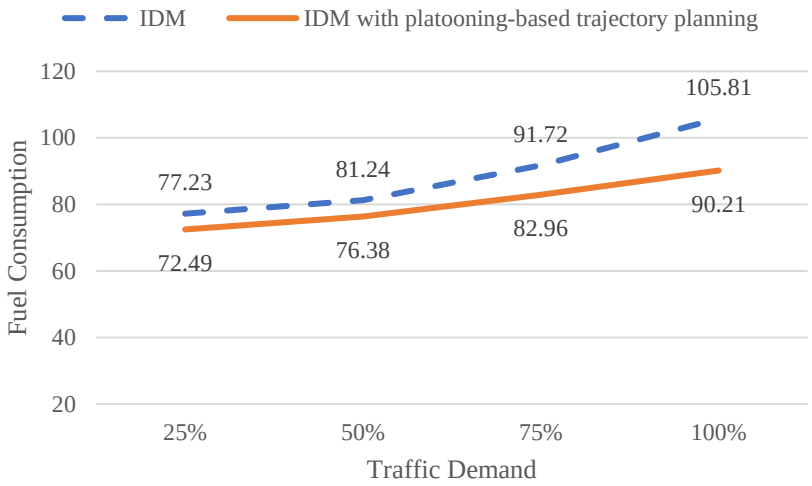

FIGURE 4.2: Average fuel consumption (ml) of CAVs in the equivalent conventional intersection

4.2.1.3 Comparison between CAVs and HDVs with Calibrated W99

This research first examines the performance of the calibrated W99 model, IDM model, IDM with platooning, IDM with trajectory planning, and IDM with platooning-based trajectory under 100% peak hour traffic volume, respectively.

Although it is expected that CAVs outperform HDVs, it may not necessarily always be true in the real world. For instance, when the vehicle travels through a congested intersection, HDVs are likely to have shorter headways and practice emergency deceleration or acceleration to achieve the minimal travel time or avoid collisions, while CAVs cannot exceed the predetermined boundary of safe headway and acceleration rates. According to Figure 4.3, the results from calibrated W99 and IDM prove this assumption since they have similar average delays and fuel consumption.

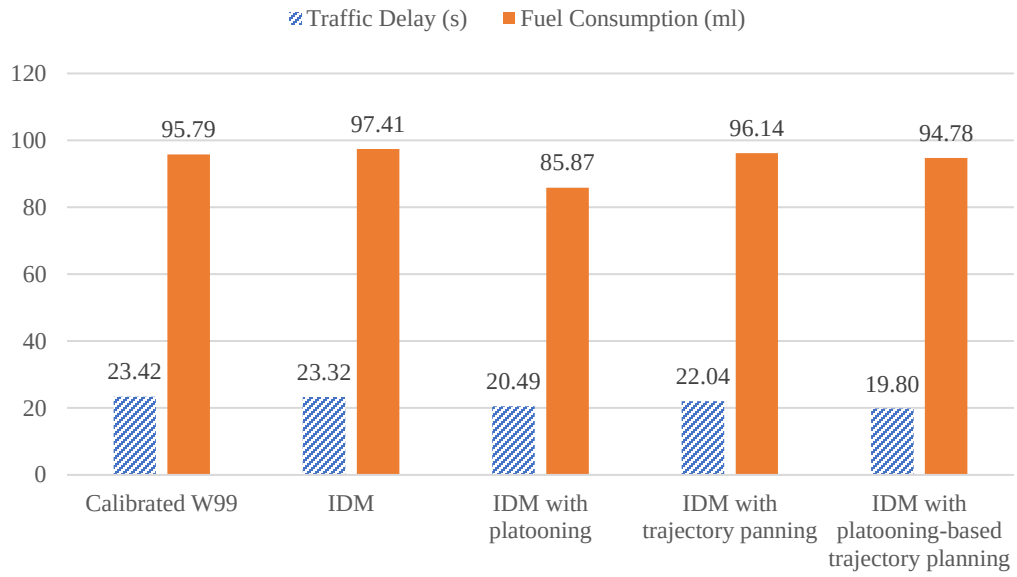

FIGURE 4.3: Traffic performances with different scenarios

However, when CAVs are enabled with platooning and trajectory planning, the CAVs may be superior to HDVs. For the proposed platooning model, compared to the IDM model, the traffic delay decreases from 23.42 to 20.49 (around 13%), while the fuel consumption decreases from 95.79 to 85.87 (around 10% reduction). Since HDVs with calibrated W99 have similar traffic delay and fuel consumption, similar improvements can be found when comparing CAV with platooning against HDVs with calibrated W99.

The outstanding performance of platooning performances may be related to the large traffic volume in this scenario. On the other hand, IDM with trajectory planning yields few benefits in terms of both traffic delay and fuel consumption compared to IDM only. As described in the previous section, CAVs will change into the car following model when they detect vehicles that are within a 3s headway. In a congested traffic condition such as 100% peak hour traffic volume, the advantages of trajectory planning are significantly compromised. As for CAVs with platooning-based trajectory planning, the traffic delay decreases and reaches the lowest traffic delay (19.80s) among all scenarios, while the fuel consumption is lower compared to CAVs with trajectory planning but higher compared to CAVs with platooning. CAVs with platooning and trajectory planning, when vehicles are close to each other, form a platoon so that trajectory planning can be executed, which explains the greater traffic delay reduction in CAVs with platooning-based trajectory planning. The fuel consumption of platooning-based trajectory planning is higher than ones of platooning but lower than the ones of trajectory planning.

4.2.2 The Performances of CAVs in Superstreets

4.2.2.1 Traffic Delay

Figure 4.4 presents the average traffic delay when CAVs are enabled with platooning, trajectory planning, and platooning-based trajectory planning. CAVs with platooning have similar performances as they did in the equivalent conventional intersection. When the traffic scale is at 25% peak hour traffic volume, the CAVs with platooning fail to reduce the average traffic delay. Nevertheless, when the traffic demand is greater or equal to 50% peak hour traffic volume, the CAVs start to reduce the traffic delay in the superstreet.

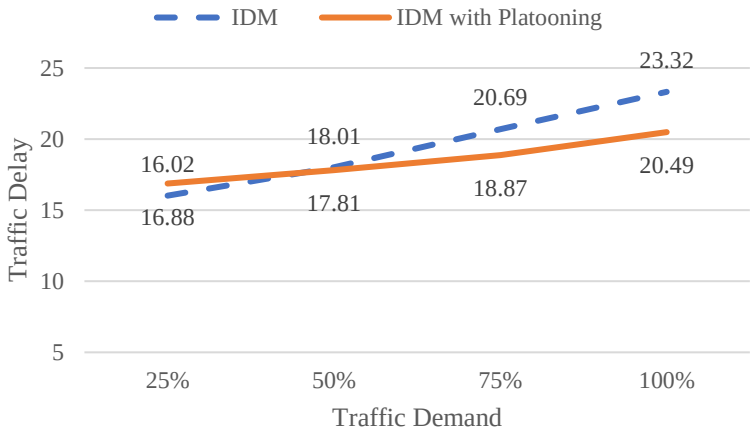

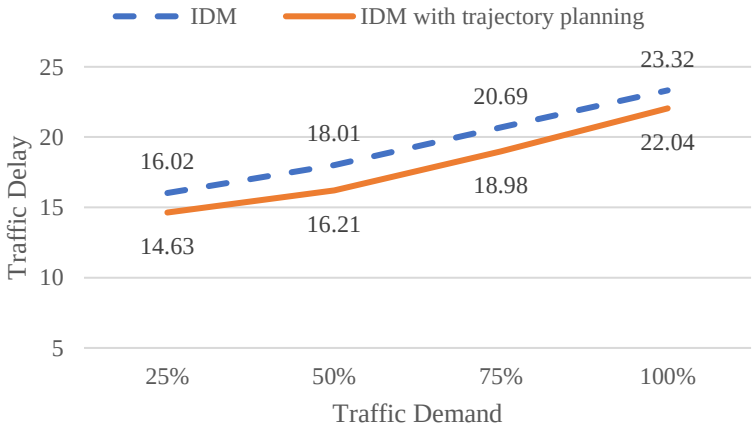

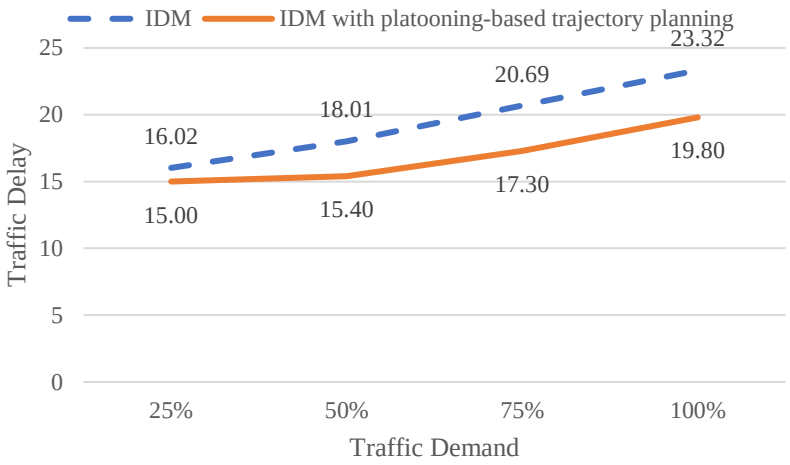

FIGURE 4.4: Average traffic delay(s) of CAVs in the superstreet

As for trajectory planning, the reductions of traffic delay with different demands are relatively constant compared to the ones in the conventional intersection. In superstreet, the road capacity often is larger than the equivalent conventional intersection. Therefore, CAVs might not have to switch to the car-following model frequently as they did in the equivalent conventional intersection in 100% peak hour traffic volume demand, which explains the relevant constant traffic delay reduction.

CAVs with platooning-based trajectory planning still produce minimal traffic delays in nearly all demand levels (except for 25% peak hour traffic demand). The general trend of traffic delays is similar to that in platooning scenarios as in the equivalent conventional intersection.

4.2.2.2 Fuel Consumption

Figure 4.5 presents the fuel consumption of CAVs in the superstreet. Platooning yields similar fuel consumption trends as it did in the traffic delay results. Nevertheless, CAVs with trajectory planning produce higher average fuel consumption, especially in the lower traffic demand scenarios. The increased average fuel consumption can be potentially attributed to two reasons: 1) the acceleration behavior of CAVs with trajectory planning in order to catch the remaining green or initiation green time; 2) CAVs with trajectory planning may stop at the second consecutive intersection after passing the first intersection with acceleration in the superstreet system. In high traffic volume scenario, the adverse effects of fuel consumption are alleviated since CAVs with trajectory planning do not have much freedom of accelerating before the intersection. This result demonstrates the necessity of incorporating information on two consecutive signals into the designing of a trajectory planning framework when two signals are closely spaced. The adverse effects on fuel consumption are alleviated when CAVs are enabled with platooning-based trajectory planning.

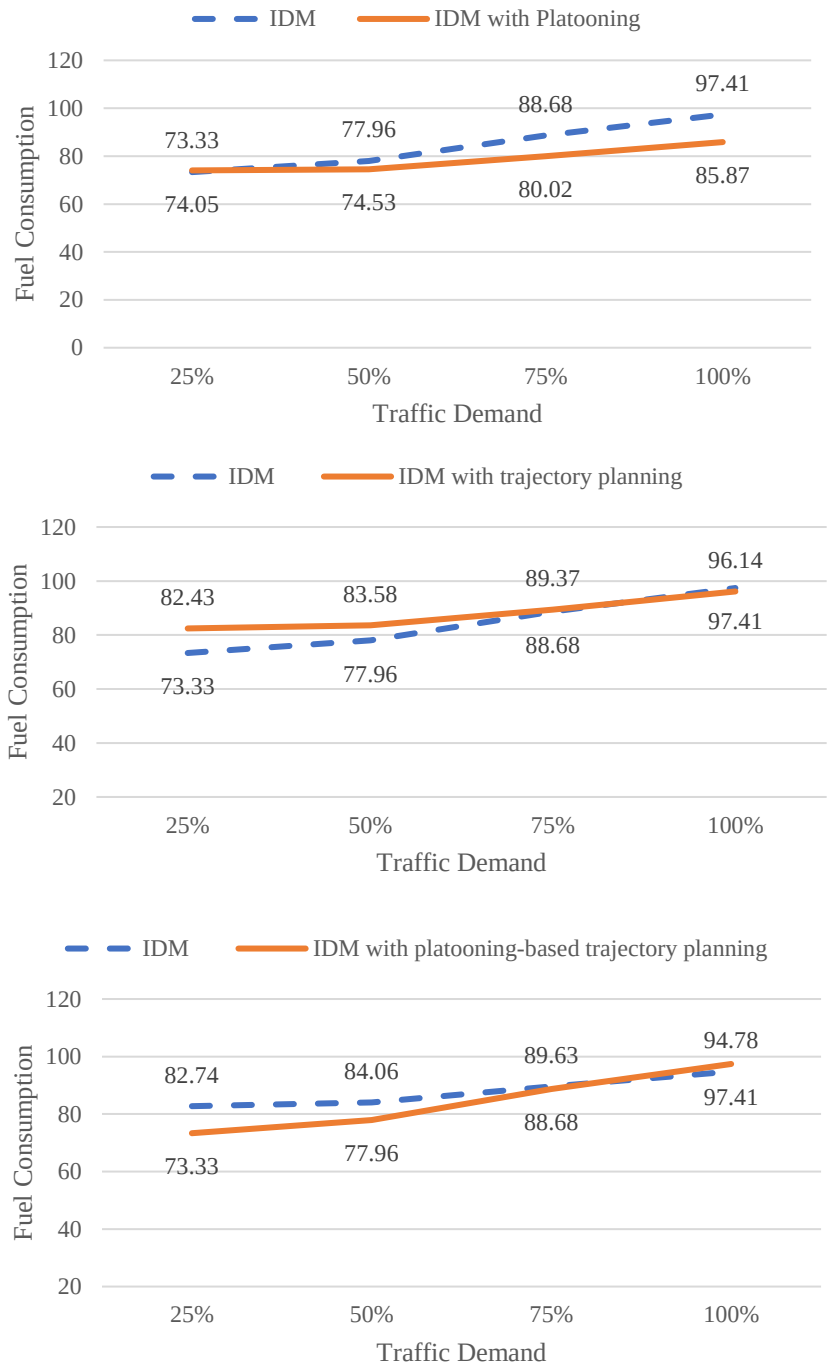

FIGURE 4.5: Average fuel consumption (ml) of CAVs in the superstreet

4.2.2.3 CAVs with Different Market Penetration Rates

The dominance of CAVs on the road is a gradual process in which technology, political and legal challenges continuously remain. The policymakers may be interested in the performances of CAVs at different levels of market penetration rates. Therefore, this research also conducts a market penetration analysis where HDVs controlled by

calibrated W99 and CAVs controlled by IDM with platooning-based trajectory planning coexist. 25%, 50%, and 75% CAV market penetration rates are tested under the 100% peak hour traffic volume. When CAVs are following HDVs, CAVs are often assumed to have a larger headway (Yu and Fan, 2018). Therefore, when CAVs are following HDVs, the CAV headway is set the same as HDVs, i.e., 1.6s. Figure 4.6 provides the results of the market penetration analysis. Based on Figure 4.6, it can be observed that traffic delay starts to fall at the market penetration of 75% CAVs where the fuel consumption is similar to that of 0% CAV. The fuel consumption and traffic delay are highest when the market penetration rate of CAVs is at the 50% level. Overall, the more mixed the vehicle types are (i.e., equal market penetration rate of CAVs and HDVs), the worse the traffic performance is.

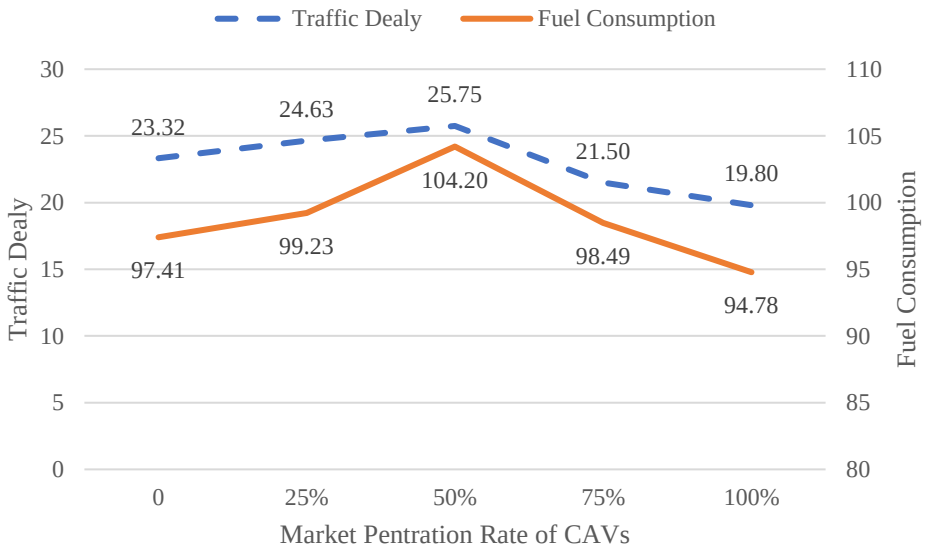

FIGURE 4.6: Analysis for different CAV market penetration rates

4.2.3 A Comparison between Conventional Intersection and Superstreet

Figure 4.7 and Figure 4.8 compare the average traffic delay and fuel consumption of CAVs in the equivalent conventional intersection and superstreet, respectively. Based on Figure 4.7, with IDM vehicles, the superstreet can consistently outperform equivalent conventional intersection regarding average traffic delay. However, it could also be observed that the average traffic delay differences between the conventional intersection and superstreet are reduced in platooning and platooning-based trajectory planning scenarios.

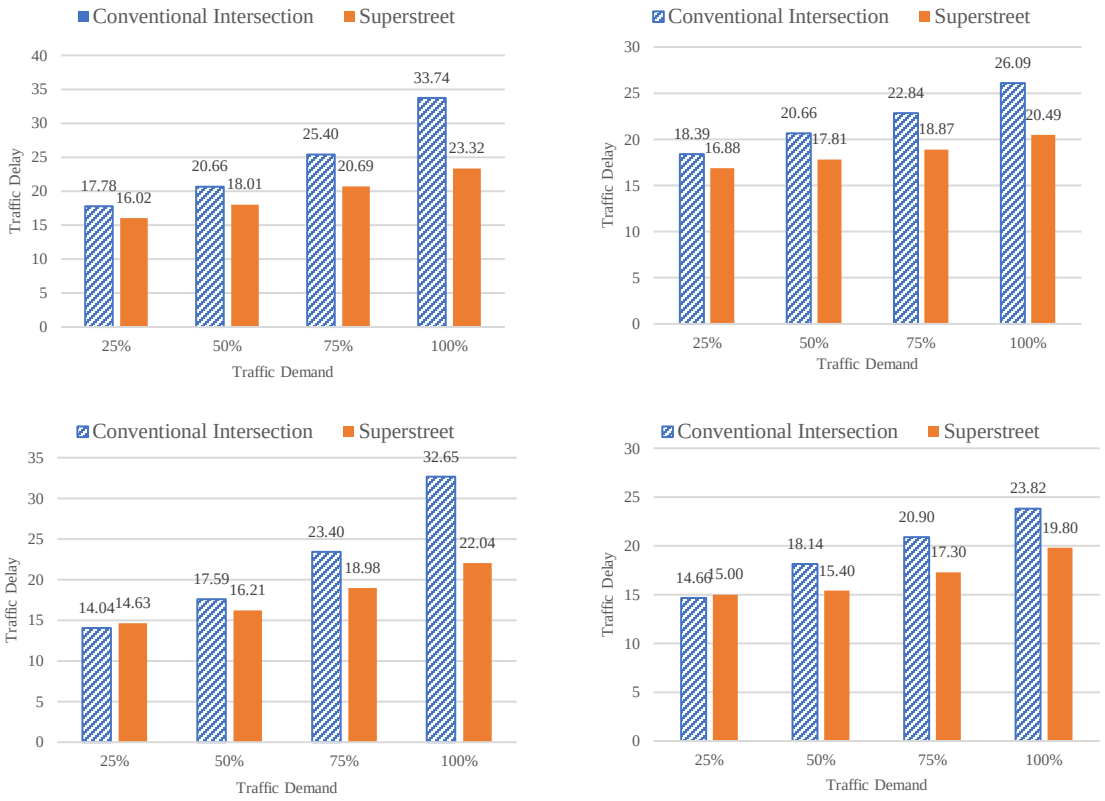

FIGURE 4.7: Average traffic delay(s) comparison of CAVs between the conventional intersection and superstreet

As for fuel consumption, Figure 4.8 shows that the average fuel consumptions of CAVs with trajectory planning are higher when they are in the superstreet under 25% and 50% peak hour traffic volume. When CAVs are enabled with platooning-based trajectory planning, they have higher average fuel consumption on all demand levels in the superstreet. As explained in the previous section, this may potentially result from the lack of consideration on two closely spaced signalized intersections when developing the trajectory planning control framework.

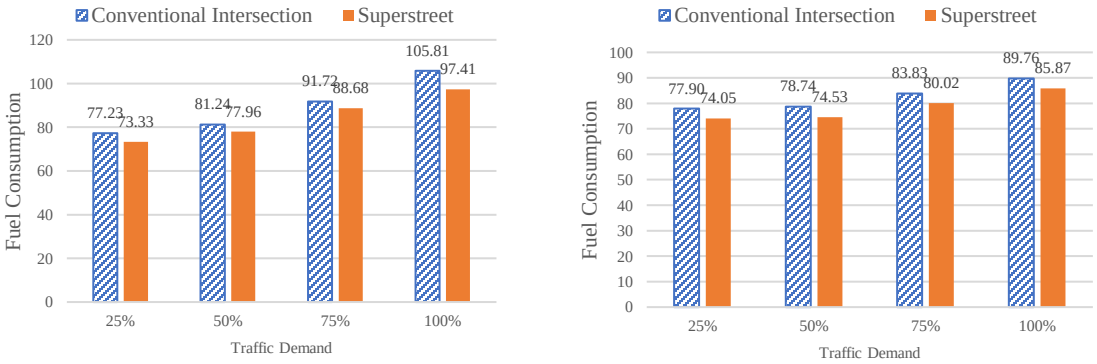

a. IDM

b. IDM with platooning

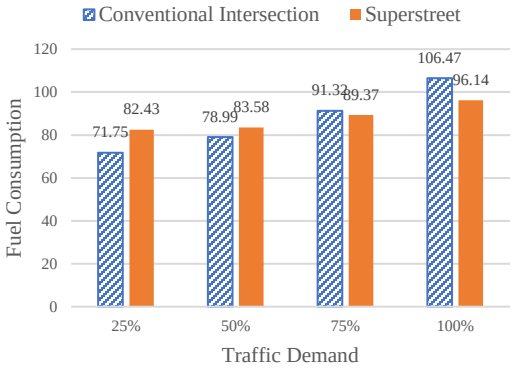

c. IDM with trajectory planning

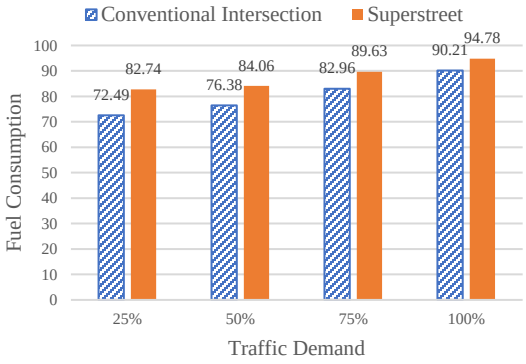

d. IDM with platooning-based trajectory planning

FIGURE 4.8: Average fuel consumption(ml) comparison of CAVs between the conventional intersection and superstreet

4.3 Platooning Control II and Adaptive Signal Control

4.3.1 Platooning Control II

The platooning control system is designed primarily to maintain a constant close distance, and the fuel consumption may increase when the following vehicles accelerate to achieve a small headway. Nevertheless, the fuel consumption and traffic delay are expected to be reduced when CAV platoons allow more vehicles to traverse the intersection given the short green signal duration. The simulation results for CAV with and without platooning control under a fixed signal timing control are presented in Table 4.1 and Table 4.2. When CAVs are equipped with platooning control, average traffic delay is reduced for both superstreet and conventional intersections. They also show a similar increasing trend of improvement magnitudes as the traffic volume increases. This is expected since when there are more vehicles, there are more chances that platooning control can take effect. The fuel consumption benefits are relatively less significant for these two environments but still show a similar trend. A notable result is that, with light traffic volumes, platooning can still yield fuel consumption reduction (1%) in superstreet but not in the conventional intersection (-1%). The reason for this slight difference is most likely to be the multiple signalized intersections for vehicles to travel through in the superstreet environment. When multiple intersections are present, CAVs have less chance to burn gasoline to accelerate even in platooning control systems. When the traffic volume is 100% peak hour volume, the equivalent conventional intersection is far more congested than the superstreet, therefore, platooning can deliver more improvements in terms of traffic delay and fuel consumption.

TABLE 4.1: CAVs With and Without Platooning in the Superstreet

Traffic Scale	**25%**		**50%**		**75%**		**100%**	
Control	With Platooning	No Platooning	With Platooning	No Platooning	With Platooning	No Platooning	With Platooning	No Platooning
TD (s)	16.10	16.77	16.09	18.22	16.60	20.78	18.32	24.42
Improvement	**4%**		**12%**		**20%**		**25%**	
FC (ml)	73.46	74.37	77.83	79.15	88.49	92.67	98.71	104.17
Improvement	**1%**		**2%**		**5%**		**5%**	

TABLE 4.2: CAVs With and Without Platooning in the Equivalent Conventional Intersection

Traffic Scale	**25%**		**50%**		**75%**		**100%**	
Control	With Platooning	No Platooning	With Platooning	No Platooning	With Platooning	No Platooning	With Platooning	No Platooning
TD (s)	16.81	17.50	18.42	20.85	19.75	24.87	21.14	32.92
Improvement	**4%**		**12%**		**21%**		**36%**	
FC (ml)	79.56	78.94	83.67	83.40	92.39	95.43	100.37	110.41
Improvement	**-1%**		**0%**		**3%**		**9%**	

4.3.2 Adaptive Signal Control

Figure 4.9 presents the traffic delay and fuel consumption reductions when the adaptive signal control in Section 3.5.1 and Section 3.5.2 is implemented. The proposed signal timing strategy can yield significant benefits in terms of both traffic delay and fuel consumption. The highest traffic delay reaches up to 75% when light traffic volume is present. As for the fuel consumption, the reduction ranges from 9% to 17% in different traffic scales. A general trend is that the improvement magnitudes decrease as the traffic volume increases in superstreet.

Figure 4.10 shows the effects of proposed signal timing with CAVs in the environment of conventional intersection. It can be easily seen that the optimized signal timing with CAVs also has a good performance, and the performance also deteriorates as the traffic volumes increase in the conventional intersection. The better performance observed in the superstreet may be attributed to the fact that superstreet have fewer conflicting movements in the intersections, which gives more flexibility in signal optimization.

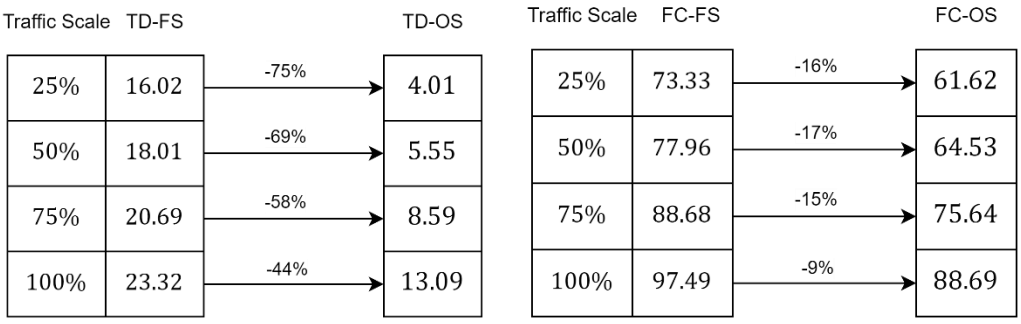

FIGURE 4.9: Comparison between fixed signal (FS) timing and optimized signal (OS) timing with CAVs in terms of traffic delay and fuel consumption in the superstreet

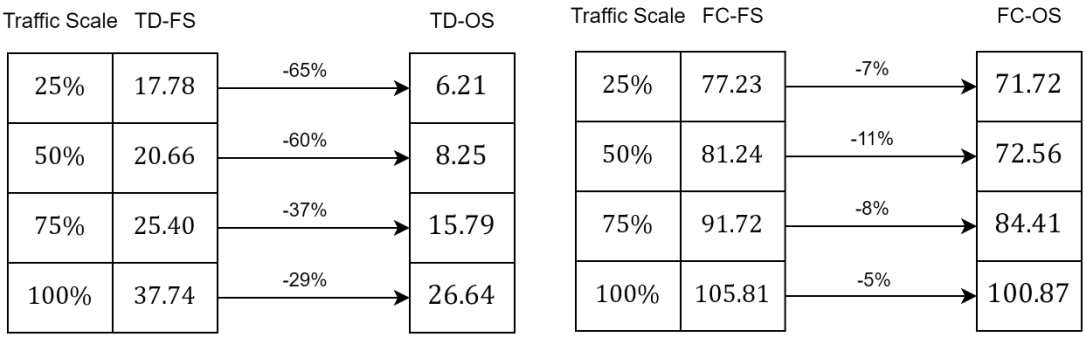

FIGURE 4.10: Comparison between fixed signal (FS) timing and optimized signal (OS) timing with CAVs in terms of traffic delay and fuel consumption in the equivalent conventional intersection

Adaptive Signal Control in Superstreet with Different Arm Length

Superstreet presents various forms in the real world to suit local needs. Therefore, it is necessary to test whether the signal timing optimization can have consistently good performance with different configurations. With the same lane configuration and traffic volume information being provided in Table 3.4, this research tests different arm lengths for the minor intersections in superstreet (original length for minor street is about $150m$ and for main street it is about $250m$). According to Table 4.3, the proposed signal control can have stable performances in different arm lengths for superstreet.

TABLE 4.3: Adaptive Signal Control with Different Arm Lengths in Superstreet

		FS	OS	Improvement
200m	TD	24.26	14.87	38%
	FC	93.64	86.44	8%
300m	TD	25.37	15.33	40%
	FC	115.59	106.61	8%
400m	TD	26.79	15.93	41%
	FC	141.06	130.94	7%

4.3.3 Trajectory Planning II under Adaptive Signal Control

Table 4.4 presents the average traffic delay and fuel consumption results with and without trajectory planning (denoted as TP in Table 4.4 and Table 4.5) under signal optimization in superstreet. The improvement magnitudes are decreasing when the traffic scale becomes larger. This is understandable since the trajectory planning module needs to be switched back to the default car following model frequently when CAVs encounter preceding vehicles in medium/high traffic volumes. The improvement magnitudes drop from 7% to 0% when traffic volumes increase from 25% to 100%. The fuel consumption is relatively insignificant, which is likely to be attributed to the unstable traffic flow caused by multiple sub intersections in superstreet. According to Table 4.4, the equivalent conventional intersection has relatively more advantages as the traffic flow is

more stable due to fewer intersections. The reduction in traffic delay shows a similar trend as it is in superstreet. The highest improvement for conventional intersection reaches 12% in terms of traffic delay in low traffic volume scenarios. The fuel consumption reduction brought by trajectory planning is as slight as 1-3%, which is still better than it does in superstreet.

TABLE 4.4: Traffic Delay and Fuel Consumption for CAVs With and Without TP Under Signal Optimization in Superstreet

Traffic Scale	**25%**		**50%**		**75%**		**100%**	
Control	With TP	No TP	With TP	No TP	With TP	No TP	With TP	No TP
TD (s)	3.85	4.13	5.32	5.59	9.00	9.06	13.75	13.81
Improvement	**7%**		**5%**		**0%**		**0%**	
FC (ml)	61.63	61.37	66.00	66.24	80.47	80.49	95.36	94.69
Improvement	**0%**		**0%**		**0%**		**0%**	

TABLE 4.5: Traffic Delay and Fuel Consumption for CAVs With and Without TP Under Signal Optimization in Conventional Intersection

Traffic Scale	**25%**		**50%**		**75%**		**100%**	
Control	With TP	No TP	With TP	No TP	With TP	No TP	With TP	No TP
TD (s)	5.5	6.12	8.54	9.26	16.07	17.42	26.91	27.86
Improvement	**10%**		**8%**		**8%**		**3%**	
FC (ml)	70.44	71.37	73.48	75.07	85.63	89.41	105.44	107.13
Improvement	**1%**		**2%**		**3%**		**2%**	

4.4 Platooning and Trajectory Planning Approach Comparison

This section compares two sets of platooning controls and trajectory planning controls. Since two sets of platooning controls and trajectory planning controls have different assumptions and model structures, this section only discusses the improvement magnitudes. Figure 4.11 and Figure 4.12 show the improvement magnitudes of traffic delays and fuel consumption between two platooning controls in the conventional intersection and superstreet. Platooning control II clearly has better performances in terms of traffic delay but not fuel consumption. This may be attributed to more acceleration behaviors to maintain small headways when vehicles leave the intersections in platooning control II. Figure 4.13 and Figure 4.14 show the comparison between trajectory planning I and trajectory planning II in terms traffic delay and fuel consumption respectively. For trajectory planning controls, trajectory planning control I shows superiority in terms of traffic delay but not fuel consumption, which is understandable as the trajectory planning control II does not consider the deceleration cases to avoid unstable traffic flows. Unstable traffic flows are likely to cause fuel consumption to increase in trajectory planning control I.

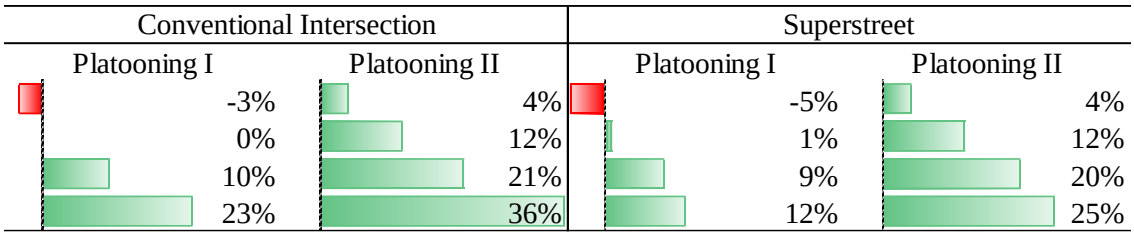

FIGURE 4.11: Traffic delay improvement magnitudes between two platooning controls

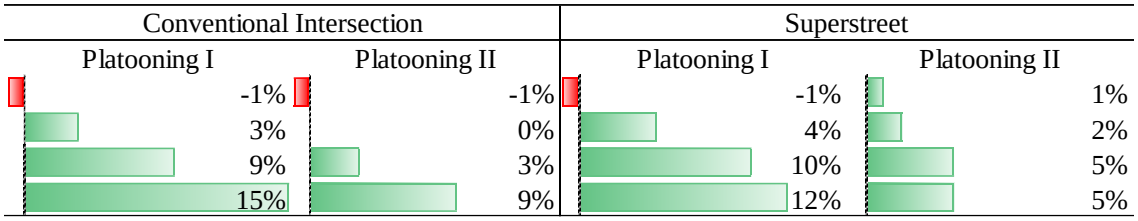

FIGURE 4.12: Fuel consumption improvement magnitudes between two platooning controls

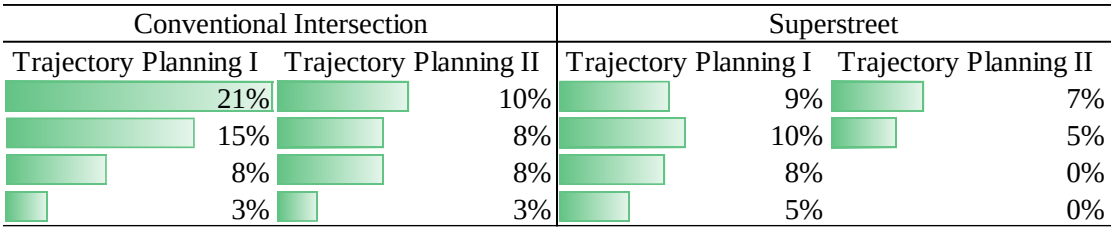

FIGURE 4.13: Traffic delay improvement magnitudes between two trajectory planning controls

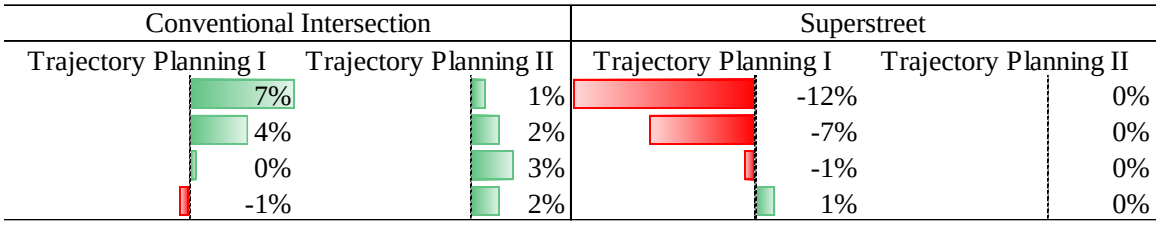

FIGURE 4.14: Fuel consumption improvement magnitudes between two trajectory planning controls

CHAPTER 5 CONCLUSIONS

5.1 Summary of Research Findings

This research investigated the performances of CAVs and HDVs in the environments of the superstreet and conventional intersection. CAVs were modeled with the IDM car-following model while HDVs were modeled with the W99 car-following model. A real-world superstreet situated in Leeland, NC, was replicated in the simulation platform to test the performances of CAVs and HDVs under different traffic conditions. In addition, to fully examine the potentiality of CAVs, platooning control, adaptive signal control, and trajectory planning strategy were developed for CAVs respectively. In this research, the W99 model was calibrated with GA so that the W99 model could better represent the local drivers' behaviors.

5.1.1 Platooning Control I and Trajectory Planning I at Fixed Signal Timing

The simulation results indicated that, without platooning and trajectory planning, CAV modeled by IDM did not have significant improvement compared to HDVs modeled by W99. The developed platooning strategy can successfully reduce the traffic delay and fuel consumption at relatively high traffic demand scenarios (50%, 75%, and 100% peak hour volume) in both the superstreet and the conventional intersection. Trajectory planning could reduce the traffic delay in both superstreet and conventional intersection environments but with different impacts on fuel consumption. CAVs with trajectory planning produced higher fuel consumption in the superstreet in the lower traffic demand scenarios, especially in traffic demand 25% and 50% of peak hour traffic volume. A potential reason was that CAVs that accelerate to pass the first intersection may fail to pass the consecutive second intersection in the environment of superstreet. In the market penetration rate analysis of CAVs, it was found that the mixed traffic environment can compromise the benefit when the CAVs market penetration rates were at 25% and 50% peak hour traffic volume. CAVs had better performances when the market penetration rate was about 75% and above.

This research also compared the traffic performances of CAVs in the conventional intersection and superstreet. A notable finding was that the proposed trajectory planning control strategy can successfully reduce the average traffic delay without increasing the average fuel consumption in the conventional intersection. This was different from superstreet where CAVs enabled with trajectory planning increase the fuel consumption. This demonstrated the efficiency of the proposed trajectory planning strategy in an isolated intersection. However, this result also indicated that the trajectory planning without considering special features of two closely spaced signalized intersections may suffer adverse effects of fuel consumption. Overall, the improvement magnitude of platooning and trajectory planning was larger than that in the conventional intersection.

5.1.2 Platooning Control II and Adaptive Signal Control

The research findings suggested that adaptive signal control with CAVs could yield the largest improvement compared to trajectory planning and platooning in terms of both traffic delay and fuel consumption; the improvement rates showed an increasing trend as the traffic scales rise. Platooning control could also yield traffic delay and fuel consumption benefits, and the highest improvement was more than 30% in terms of traffic delay in 100% peak hour traffic volume. In contrast to platooning and adaptive signal control, the effects of trajectory planning were attenuated when the traffic volume increases, which are understandable since CAVs must stop following predetermined trajectories when encountering close preceding vehicles. The unstable traffic flow caused by multiple intersections made the improvement for fuel consumption even less significant in the environment of superstreet. For most cases, performances of CAVs with different features showed a similar trend in the equivalent conventional intersection as they were in superstreet. CAV with trajectory planning performed better in conventional intersection design while CAVs with adaptive signal control performed better in superstreet. Table 5.1 provides a summary for performance comparison with different CAV techniques.

TABLE 5.1: A Summary on the Environment of Greater Improvement for Different CAV Techniques

	TD		FC	
	Light Traffic	**Heavy Traffic**	**Light Traffic**	**Heavy Traffic**
Platooning control I	Similar	Conventional Intersection	Superstreet	Conventional Intersection
Adaptive Signal Control	Superstreet	Superstreet	Superstreet	Superstreet
Trajectory Planning II Under Adaptive Signal Control	Conventional Intersection	Conventional Intersection	Conventional Intersection	Conventional Intersection

5.2 Future Research Direction Discussions

Based on these research findings, future research directions could be the adaptive signal control strategy that takes arrival information on CAVs into consideration, which may reduce the adverse effects of trajectory planning on fuel consumption identified in this research. Also, a more sophisticated trajectory planning algorithm that accounts for two consecutive signalized intersections can be developed.

REFERENCES

Adebisi, Adekunle, et al. "Developing highway capacity manual capacity adjustment factors for connected and automated traffic on freeway segments." Transportation Research Record 2674.10 (2020): 401-415.

Ahmed, H. U., Huang, Y., & Lu, P. (2021). A review of car-following models and modeling tools for human and autonomous-ready driving behaviors in micro-simulation. *Smart Cities*, *4*(1), 314-335.

Anil Chaudhari, A., Srinivasan, K. K., Rama Chilukuri, B., Treiber, M., & Okhrin, O. (2022). Calibrating Wiedemann-99 model parameters to trajectory data of mixed vehicular traffic. *Transportation research record*, 03611981211037543.

Bang, S., & Ahn, S. (2017). Platooning strategy for connected and autonomous vehicles: transition from light traffic. Transportation Research Record, 2623(1), 73-81.

Bevly, D., Murray, C., Lim, A., Turochy, R., Sesek, R., Smith, S., ... & Boyd, S. (2015). Heavy truck cooperative adaptive cruise control: evaluation, testing, and stakeholder engagement for near term deployment: phase one final report.

Bhoopalam, A. K., Agatz, N., & Zuidwijk, R. (2018). Planning of truck platoons: A literature review and directions for future research. Transportation research part B: methodological, 107, 212-228.

Bian, Y., Zheng, Y., Ren, W., Li, S. E., Wang, J., & Li, K. (2019). Reducing time headway for platooning of connected vehicles via V2V communication. Transportation Research Part C: Emerging Technologies, 102, 87-105.

Bifulco, G. N., Pariota, L., Simonelli, F., & Di Pace, R. (2013). Development and testing of a fully adaptive cruise control system. Transportation Research Part C: Emerging Technologies, 29, 156-170.

Chalaki, B., Beaver, L. E., & Malikopoulos, A. A. (2020, October). Experimental validation of a real-time optimal controller for coordination of CAVs in a multi-lane roundabout. In 2020 IEEE Intelligent Vehicles Symposium (IV) (pp. 775-780). IEEE.

Chen, D., Laval, J., Zheng, Z., & Ahn, S. (2012). A behavioral car-following model that captures traffic oscillations. Transportation research part B: methodological, 46(6), 744-761.

Cheng, Y., Hu, X., Chen, K., Yu, X., & Luo, Y. (2022). Online longitudinal trajectory planning for connected and autonomous vehicles in mixed traffic flow with deep reinforcement learning approach. *Journal of Intelligent Transportation Systems*, 1-15.

Chityala, S., Sobanjo, J. O., Erman Ozguven, E., Sando, T., & Twumasi-Boakye, R. (2020). Driver behavior at a freeway merge to mixed traffic of conventional and connected autonomous vehicles. Transportation research record, 2674(11), 867-874.

Daganzo, C. F. (1994). The cell transmission model: A dynamic representation of highway traffic consistent with the hydrodynamic theory. Transportation Research Part B: Methodological, 28(4), 269-287.

Daganzo, C. F. (1995). The cell transmission model, part II: network traffic. Transportation Research Part B: Methodological, 29(2), 79-93.

Darbha, S., Konduri, S., & Pagilla, P. R. (2017, May). Effects of V2V communication on time headway for autonomous vehicles. In 2017 American control conference (ACC) (pp. 2002-2007). IEEE.

Darbha, S., Konduri, S., & Pagilla, P. R. (2018). Benefits of V2V communication for autonomous and connected vehicles. IEEE Transactions on Intelligent Transportation Systems, 20(5), 1954-1963.

Derbel, O., Peter, T., Zebiri, H., Mourllion, B., & Basset, M. (2013). Modified intelligent driver model for driver safety and traffic stability improvement. IFAC Proceedings Volumes, 46(21), 744-749.

Ding, C., Dai, R., Fan, Y., Zhang, Z., & Wu, X. (2021). Collaborative control of traffic signal and variable guiding lane for isolated intersection under connected and automated vehicle environment. Computer-Aided Civil and Infrastructure Engineering.

Durrani, U., Lee, C., & Maoh, H. (2016). Calibrating the Wiedemann's vehicle-following model using mixed vehicle-pair interactions. *Transportation research part C: emerging technologies*, *67*, 227-242.

Feng, Y., Yu, C., & Liu, H. X. (2018). Spatiotemporal intersection control in a connected and automated vehicle environment. Transportation Research Part C: Emerging Technologies, 89, 364-383.

Geiger, A., Lauer, M., Moosmann, F., Ranft, B., Rapp, H., Stiller, C., & Ziegler, J. (2012). Team AnnieWAY's entry to the 2011 grand cooperative driving challenge. IEEE Transactions on Intelligent Transportation Systems, 13(3), 1008-1017.

Gong, S., & Du, L. (2018). Cooperative platoon control for a mixed traffic flow including human drive vehicles and connected and autonomous vehicles. *Transportation research part B: methodological*, *116*, 25-61.

Gong, S., Shen, J., & Du, L. (2016). Constrained optimization and distributed computation based car following control of a connected and autonomous vehicle platoon. Transportation Research Part B: Methodological, 94, 314-334.

Gong, S., Shen, J., & Du, L. (2016). Constrained optimization and distributed computation based car following control of a connected and autonomous vehicle platoon. *Transportation Research Part B: Methodological*, *94*, 314-334.

Guo, Y., & Ma, J. (2020). Leveraging existing high-occupancy vehicle lanes for mixed-autonomy traffic management with emerging connected automated vehicle applications. Transportmetrica A: Transport Science, 16(3), 1375-1399.

Guo, Y., Ma, J., Xiong, C., Li, X., Zhou, F., & Hao, W. (2019). Joint optimization of vehicle trajectories and intersection controllers with connected automated vehicles: Combined dynamic programming and shooting heuristic approach. Transportation research part C: emerging technologies, 98, 54-72.

Guo, Y., & Ma, J. (2021). SCoPTO: signalized corridor management with vehicle platooning and trajectory control under connected and automated traffic environment. *Transportmetrica B: Transport Dynamics*, *9*(1), 673-692.

Haley, R. L., Ott, S. E., Hummer, J. E., Foyle, R. S., Cunningham, C. M., & Schroeder, B. J. (2011). Operational effects of signalized superstreets in North Carolina. Transportation Research Record, 2223(1), 72-79.

Hallé, S., & Chaib-draa, B. (2005). A collaborative driving system based on multiagent modelling and simulations. *Transportation Research Part C: Emerging Technologies*, *13*(4), 320-345.

Han, X., Ma, R., & Zhang, H. M. (2020). Energy-aware trajectory optimization of CAV platoons through a signalized intersection. *Transportation Research Part C: Emerging Technologies*, *118*, 102652.

He, Y., Ciuffo, B., Zhou, Q., Makridis, M., Mattas, K., Li, J., ... & Xu, H. (2019). Adaptive cruise control strategies implemented on experimental vehicles: A review. IFAC-PapersOnLine, 52(5), 21-27.

Hummer, J., Haley, R. L., Ott, S. E., Foyle, R. S., & Cunningham, C. M. (2010). Superstreet benefits and capacities. Department of Civil, Construction and Environmental Engineering, North Carolina State University, Raleigh, NC.

Hummer, J., Ray, B., Daleiden, A., Jenior, P., & Knudsen, J. (2014). Restricted crossing U-turn: informational guide (No. FHWA-SA-14-070). United States. Federal Highway Administration. Office of Safety.

Hurtado-Beltran, A., & Rilett, L. R. (2021). Impact of CAV Truck Platooning on HCM-6 Capacity and Passenger Car Equivalent Values. *Journal of Transportation Engineering, Part A: Systems*, *147*(2), 04020159.

Hu, X., & Sun, J. (2019). Trajectory optimization of connected and autonomous vehicles at a multilane freeway merging area. Transportation Research Part C: Emerging Technologies, 101, 111-125.

Kamalanathsharma, R. K., Rakha, H. A., & Yang, H. (2015). Networkwide impacts of vehicle ecospeed control in the vicinity of traffic signalized intersections. Transportation Research Record, 2503(1), 91-99.

Kaths, H., Keler, A., & Bogenberger, K. (2021). Calibrating the wiedemann 99 car-following model for bicycle traffic. Sustainability, 13(6), 3487.

Kesting, A., & Treiber, M. (2008). Calibrating car-following models by using trajectory data: Methodological study. Transportation Research Record, 2088(1), 148-156.

Koshal, J., Nedić, A., & Shanbhag, U. V. (2011). Multiuser optimization: Distributed algorithms and error analysis. SIAM Journal on Optimization, 21(3), 1046-1081.

Li, N., Chen, S., Zhu, J., & Sun, D. J. (2020). A platoon-based adaptive signal control method with connected vehicle technology. Computational intelligence and neuroscience, 2020.

Li, N., Chen, S., Zhu, J., & Sun, D. J. (2020). A platoon-based adaptive signal control method with connected vehicle technology. Computational intelligence and neuroscience, 2020.

Li, P. T., & Zhou, X. (2017). Recasting and optimizing intersection automation as a connected-and-automated-vehicle (CAV) scheduling problem: A sequential branch-and-bound search approach in phase-time-traffic hypernetwork. Transportation Research Part B: Methodological, 105, 479-506.

Li, P., Mirchandani, P., & Zhou, X. (2015). Solving simultaneous route guidance and traffic signal optimization problem using space-phase-time hypernetwork. Transportation Research Part B: Methodological, 81, 103-130.

Liang, X., Guler, S. I., & Gayah, V. V. (2018). Signal timing optimization with connected vehicle technology: Platooning to improve computational efficiency. *Transportation Research Record*, *2672*(18), 81-92.

Lin, W. H., & Wang, C. (2004). An enhanced 0-1 mixed-integer LP formulation for traffic signal control. IEEE Transactions on Intelligent transportation systems, 5(4), 238-245.

Liu, H., Kan, D. K., Shladover, S., Lu, X. Y., Wang, M., Schakel, W., & van Aren, B. (2018). *Using cooperative adaptive cruise control (CACC) to form high-performance vehicle streams*. California PATH Progam, Institute of Transportation Studies, University of California, Berkeley.

Liu, P., & Fan, W. Exploring the impact of connected and autonomous vehicles on freeway capacity using a revised Intelligent Driver Model. *Transportation planning and technology*, 2020. 43(3), 279-292.

Lo, H. K. (1999). A novel traffic signal control formulation. Transportation Research Part A: Policy and Practice, 33(6), 433-448.

Lo, H. K. (2001). A cell-based traffic control formulation: strategies and benefits of dynamic timing plans. Transportation Science, 35(2), 148-164.

Ma, J., Li, X., Zhou, F., Hu, J., & Park, B. B. (2017). Parsimonious shooting heuristic for trajectory design of connected automated traffic part II: computational issues and optimization. *Transportation Research Part B: Methodological*, *95*, 421-441.

Malinauskas, R. M. (2014). The intelligent driver model: Analysis and application to adaptive cruise control (Doctoral dissertation, Clemson University).

Martin-Gasulla, M., & Elefteriadou, L. (2021). Traffic management with autonomous and connected vehicles at single-lane roundabouts. Transportation research part C: emerging technologies, 125, 102964.

Milanés, V., & Shladover, S. E. (2014). Modeling cooperative and autonomous adaptive cruise control dynamic responses using experimental data. Transportation Research Part C: Emerging Technologies, 48, 285-300.

Mohebifard, R., & Hajbabaie, A. (2020, September). Effects of automated vehicles on traffic operations at roundabouts. In 2020 IEEE 23rd International Conference on Intelligent Transportation Systems (ITSC) (pp. 1-6). IEEE.

Mohebifard, R., & Hajbabaie, A. (2021). Trajectory control in roundabouts with a mixed fleet of automated and human-driven vehicles. Computer-Aided Civil and Infrastructure Engineering

Moon, S., Moon, I., & Yi, K. (2009). Design, tuning, and evaluation of a full-range adaptive cruise control system with collision avoidance. Control Engineering Practice, 17(4), 442-455.

Naghawi, H. H., & Idewu, W. I. A. (2014). Analyzing delay and queue length using microscopic simulation for the unconventional intersection design Superstreet. Journal of the South African Institution of Civil Engineering, 56(1), 100-107.

Naghawi, H., AlSoud, A., & AlHadidi, T. (2018). The possibility for implementing the superstreet unconventional intersection design in Jordan. Periodica Polytechnica Transportation Engineering, 46(3), 122-128.

Nowakowski, C., O'Connell, J., Shladover, S. E., & Cody, D. (2010, September). Cooperative adaptive cruise control: Driver acceptance of following gap settings less than one second. In Proceedings of the Human Factors and Ergonomics Society Annual Meeting (Vol. 54, No. 24, pp. 2033-2037). Sage CA: Los Angeles, CA: SAGE Publications.

Olstam, J. J., & Tapani, A. (2004). *Comparison of Car-following models* (Vol. 960). Linköping: Swedish National Road and Transport Research Institute.

Ott, S. E., Fiedler, R. L., Hummer, J. E., Foyle, R. S., & Cunningham, C. M. (2015). Resident, Commuter, and Business Perceptions of New Superstreets. Journal of Transportation Engineering, 141(7), 04015003.

Paden, B., Čáp, M., Yong, S. Z., Yershov, D., & Frazzoli, E. (2016). A survey of motion planning and control techniques for self-driving urban vehicles. IEEE Transactions on intelligent vehicles, 1(1), 33-55.

Ploeg, J., Semsar-Kazerooni, E., Lijster, G., van de Wouw, N., & Nijmeijer, H. (2014). Graceful degradation of cooperative adaptive cruise control. IEEE Transactions on Intelligent Transportation Systems, 16(1), 488-497.

Qadri, S. S. S. M., Gökçe, M. A., & Öner, E. (2020). State-of-art review of traffic signal control methods: challenges and opportunities. European transport research review, 12(1), 1-23.

Rajamani, R. (2011). Vehicle dynamics and control. Springer Science & Business Media.

Reid, J. D., & Hummer, J. E. (2001). Travel time comparisons between seven unconventional arterial intersection designs. Transportation Research Record, 1751(1), 56-66.

Shladover, S. E. (1995). Review of the state of development of advanced vehicle control systems (AVCS). Vehicle System Dynamics, 24(6-7), 551-595.

Shladover, S. E., Su, D., & Lu, X. Y. (2012). Impacts of cooperative adaptive cruise control on freeway traffic flow. Transportation Research Record, 2324(1), 63-70.

Tajalli, M., & Hajbabaie, A. (2018). Distributed optimization and coordination algorithms for dynamic speed optimization of connected and autonomous vehicles in urban street networks. Transportation research part C: emerging technologies, 95, 497-515.

Treiber, M., & Kesting, A. (2017). The intelligent driver model with stochasticity-new insights into traffic flow oscillations. Transportation research procedia, 23, 174-187.

Treiber, M., Hennecke, A., & Helbing, D. (2000). Microscopic simulation of congested traffic. In Traffic and granular flow'99 (pp. 365-376). Springer, Berlin, Heidelberg.

Tsai, C. C., Hsieh, S. M., & Chen, C. T. (2010). Fuzzy longitudinal controller design and experimentation for adaptive cruise control and stop&go. Journal of Intelligent & Robotic Systems, 59(2), 167-189.

Van Arem, B., Van Driel, C. J., & Visser, R. (2006). The impact of cooperative adaptive cruise control on traffic-flow characteristics. IEEE Transactions on intelligent transportation systems, 7(4), 429-436.

Wan, N., Vahidi, A., & Luckow, A. (2016). Optimal speed advisory for connected vehicles in arterial roads and the impact on mixed traffic. Transportation Research Part C: Emerging Technologies, 69, 548-563.

Wang, P. S., Li, P. T., Chowdhury, F. R., Zhang, L., & Zhou, X. (2020). A mixed integer programming formulation and scalable solution algorithms for traffic control coordination across multiple intersections based on vehicle space-time trajectories. Transportation research part B: methodological, 134, 266-304.

Wei, Y., Avcı, C., Liu, J., Belezamo, B., Aydın, N., Li, P. T., & Zhou, X. (2017). Dynamic programming-based multi-vehicle longitudinal trajectory optimization with simplified car following models. *Transportation research part B: methodological*, *106*, 102-129.

Xiao, L., & Gao, F. (2011). Practical string stability of platoon of adaptive cruise control vehicles. IEEE Transactions on intelligent transportation systems, 12(4), 1184-1194.

Xiao, L., Wang, M., & Van Arem, B. (2017). Realistic car-following models for microscopic simulation of adaptive and cooperative adaptive cruise control vehicles. Transportation Research Record, 2623(1), 1-9.

Xiong, B.-K., Jiang, R., & Tian, J.-F. (2019). Improving two-dimensional intelligent driver models to overcome overly high deceleration in car-following. Physica a: Statistical Mechanics and Its Applications, 534, 122313. https://doi.org/10.1016/j.physa.2019.122313

Xu, L., Yang, X., & Chang, G. L. (2017). Computing the Minimal U-Turn Offset for an Unsignalized Superstreet. Transportation Research Record, 2618(1), 48-57.

Xu, L., Yang, X., & Chang, G. L. (2019). Two-stage model for optimizing traffic signal control plans of signalized Superstreet. Transportmetrica A: transport science, 15(2), 993-1018.

Yao, Z., Zhao, B., Yuan, T., Jiang, H., & Jiang, Y. (2020). Reducing gasoline consumption in mixed connected automated vehicles environment: A joint optimization framework for traffic signals and vehicle trajectory. *Journal of Cleaner Production*, *265*, 121836.

Ye, Q., Chen, X., Liao, R., & Yu, L. (2019). Development and evaluation of a vehicle platoon guidance strategy at signalized intersections considering fuel savings. Transportation Research Part D: Transport and Environment, 77, 120-131.

Yu, C., Feng, Y., Liu, H. X., Ma, W., & Yang, X. (2018). Integrated optimization of traffic signals and vehicle trajectories at isolated urban intersections. Transportation Research Part B: Methodological, 112, 89-112.

Zhao, W., Liu, R., & Ngoduy, D. (2021). A bilevel programming model for autonomous intersection control and trajectory planning. *Transportmetrica A: transport science*, *17*(1), 34-58.

Zhao, W., Ngoduy, D., Shepherd, S., Liu, R., & Papageorgiou, M. (2018). A platoon based cooperative eco-driving model for mixed automated and human-driven vehicles at a signalised intersection. Transportation Research Part C: Emerging Technologies, 95, 802-821.

Zhou, A., Gong, S., Wang, C., & Peeta, S. (2020). Smooth-Switching Control-Based Cooperative Adaptive Cruise Control by Considering Dynamic Information Flow Topology. Transportation Research Record, 2674(4), 444-458.

Zhou, F., Li, X., & Ma, J. (2017). Parsimonious shooting heuristic for trajectory design of connected automated traffic part I: Theoretical analysis with generalized time geography. Transportation Research Part B: Methodological, 95, 394-420.